Hemispheric Brain Tumors

Francisco J. Romero-Vidal, Arantxa Ortega-Aznar

1.3

Contents

Introduction

The incidence of brain tumors has been estimated at 4.5 per 100,000 inhabitants. In autopsy series, they are found in 2.5% of cases. In this chapter, we will analyze supratentorial hemisphere tumors of the central nervous system (CNS) in the context of the WHO criteria, published in 2000 [1].

The WHO criteria are based on a histological evaluation of the tumor cell types and tissue patterns recognized by conventional optic microscopy and include the related information gleaned from immunohistochemical studies. The importance of this classification is that besides introducing important changes, it substantially clarifies the degree of malignancy. The modifications that have been made can be summarized in the following points:

a. Introduction of new tumoral entities described in recent years such as:
   - Pleomorphic xanthoastrocytoma [2]
   - Central neurocytoma [3]
   - Dysembryoplastic neuroepithelial tumor [4]
b. However, for selective use the term "primitive neuroectodermal tumor" (PNET) is accepted for some embryonal tumors in children.
c. Changes in the consideration of astrocytic tumors and the progression of glioma to malignancy. Basically, a clear a line of separation has been drawn between circumscribed astrocytic lesions (such as pilocytic astrocytoma, pleomorphic xanthoastrocytoma and subependymal giant cell astrocytoma associated with tuberous sclerosis) and diffusely infiltrating astrocytomas, which are typically located in the cerebral hemispheres. This last group alone shows an intrinsic tendency to progress to an anaplastic astrocytoma, and finally to multiforme glioblastoma.
d. Multiform glioblastoma, one of the most frequently occurring malignant tumors in adults, has been displaced from the group of embryonal tumors to group of astrocytic tumors. Presently multiforme glioblastoma is considered to be the extreme of the spectrum of loss of differentiation seen in astrocytic tumors [1].
e. Astroblastoma and ependymoblastoma are considered by some authors as architectural patterns that can occur in gliomas, while others believe them to be true clinical pathological entities. To resolve this problem, they have been included in a group termed "uncertain histogenesis."
f. New histological subtypes have been recognized in the ependymomas group. The majority are not associated with a different biological behavior, but their description helps the pathologist in identifying and classifying them.
g. The entity called monstrocellular sarcoma has been eliminated.
h. Together with the indispensable element of histological typing of central nervous system tumors, a scale of increasing degree of malignancy (I to IV) has been created. In general, each type of tumor corresponds to one of these degrees. Thus, when diagnosis is established, it is not possible to apply different degrees of malignancy to the same tumor.

Tumors of Neuroepithelial Tissue

Low-Grade Diffuse Astrocytomas

Astrocytic tumors are characterized by a high degree of cellular differentiation, slow growth, and diffuse infiltration of the neighboring brain structures. These lesions, corresponding to grade II in the WHO classification, have a tendency to malignant progression [1, 6].

Low-grade fibrillary astrocytomas are neoplasms occurring in children and adults from 20–40 years of age. Fibrillary astrocytomas are found throughout the hemispheres in proportion to the white matter present, and often involve the adjacent cortex as well.

Seizures are a common presenting symptom.

Radiopathological Correlation

Because of their infiltrating nature, these low-grade astrocytomas usually show blurring of the gross anatomical boundaries on microscopy. This feature is due to enlargement and distortion, but not destruction, of the invaded anatomical structures [7].

On CT, low-grade astrocytoma is commonly visualized as a nonenhancing, poorly defined, homogeneous, low-grade density mass. However, calcification, cystic change and even varying degrees of enhancement may be present early. Surrounding edema is minimal or absent [8, 9].

MRI studies usually show hypointensity in the T1-weighted images (T1-W), with enlargement of the areas first affected by the tumor and hyperintensity on T2-W [10] (Fig. 1). Gadolinium enhancement is uncommon in low-grade diffuse astrocytoma, but it can manifest with progression of the tumor.

Anaplastic Astrocytoma

Anaplastic astrocytoma is an infiltrating lesion with local or dispersed anaplasia and a marked proliferative potential. Anaplastic astrocytomas may arise from low-grade astrocytoma, but they can also be diagnosed first, without indication of a less malignant precursor lesion. These tumors are classified as grade III in the WHO system and require two histological criteria, usually nuclear atypia and mitotic activity, to be included in this category [1, 6].

Anaplastic astrocytomas generally appear in a slightly higher age group than low-grade astrocytoma (mean, 41 years) and a predominance of males are affected (2:1). The clinical symptoms are similar to those of low-grade astrocytomas, but with a shorter history.

Radiopathological Correlation

Generally it is not possible to grossly distinguish between low-grade and anaplastic astrocytomas. On the cut surface, the high cellularity of anaplastic astrocytomas produces a discernible tumor mass, which shows a clearer distinction from the surrounding brain struc-

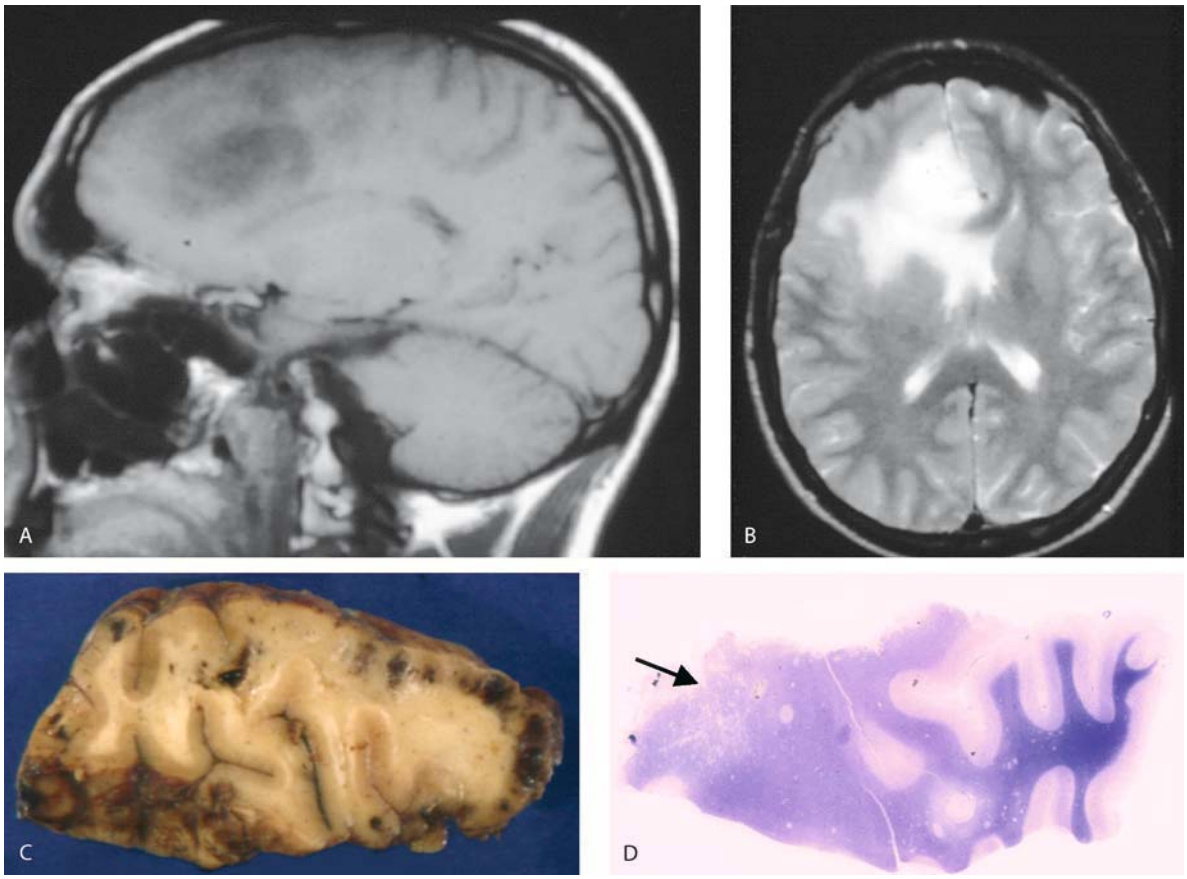

Fig. 1A–D. Low-grade diffuse astrocytoma. **A** MRI T1-W sagittal shows hypointense frontal area. **B** MI T2 W axial scan with hyperintense lesion located on the frontal white matter. **C** Coronal section of frontal lobe with a poorly defined mass and local blurring of the neocortex with focal hemorrhages. **D** Histological picture of the same section shows reduced myelin staining in white matter while the cortex shows increased cellularity with a diffuse infiltration pattern of growth (*arrow*)

tures than does low-grade diffuse astrocytoma. Macroscopic cysts are common, but frequently there are areas of granularity, opacity and a soft consistency.

On CT study, anaplastic astrocytoma tends to be nonhomogeneous and shows a mixed density. Calcifications are infrequent, except in cases of malignant transformation of a low-grade astrocytoma. Contrast uptake is heterogeneous and occasionally irregular ring enhancement is seen because of edema surrounding the lesion [9] (Fig. 2).

MRI shows a heterogeneous intensity on the T1- and T2-weighted images. On T2-W, the lesion often presents as a hyperintense area surrounded by an isointense ring which, in turn, is surrounded by a hyperintensity produced by vasogenic edema (Fig. 2A). Following contrast administration, marked but irregular peripheral ring-like enhancement is usually evident (Fig. 2B), but non-enhancing lesions may be histologically anaplastic [11]. Anaplastic astrocytoma may also spread to the ependyma, leptomeninges and cerebrospinal fluid (CSF).

Glioblastoma Multiforme

Glioblastoma multiforme, composed of poorly differentiated neoplastic astrocytes with areas of vascular proliferation and/or necrosis, is the most malignant astrocytic tumor. Glioblastoma typically affects adults and is mainly found in the cerebral hemispheres [1]. The tumors can develop from low-grade diffuse or anaplastic astrocytoma (secondary glioblastoma) (Fig. 3), but more frequently, they manifest after a short clinical history with no evidence of a less malignant precursor lesion (primary glioblastoma) [(6].

Corresponding to grade IV in the WHO system, glioblastoma requires three or four histological criteria for this classification: nuclear atypia, mitotic activity, microvascular proliferation, and/or necrosis.

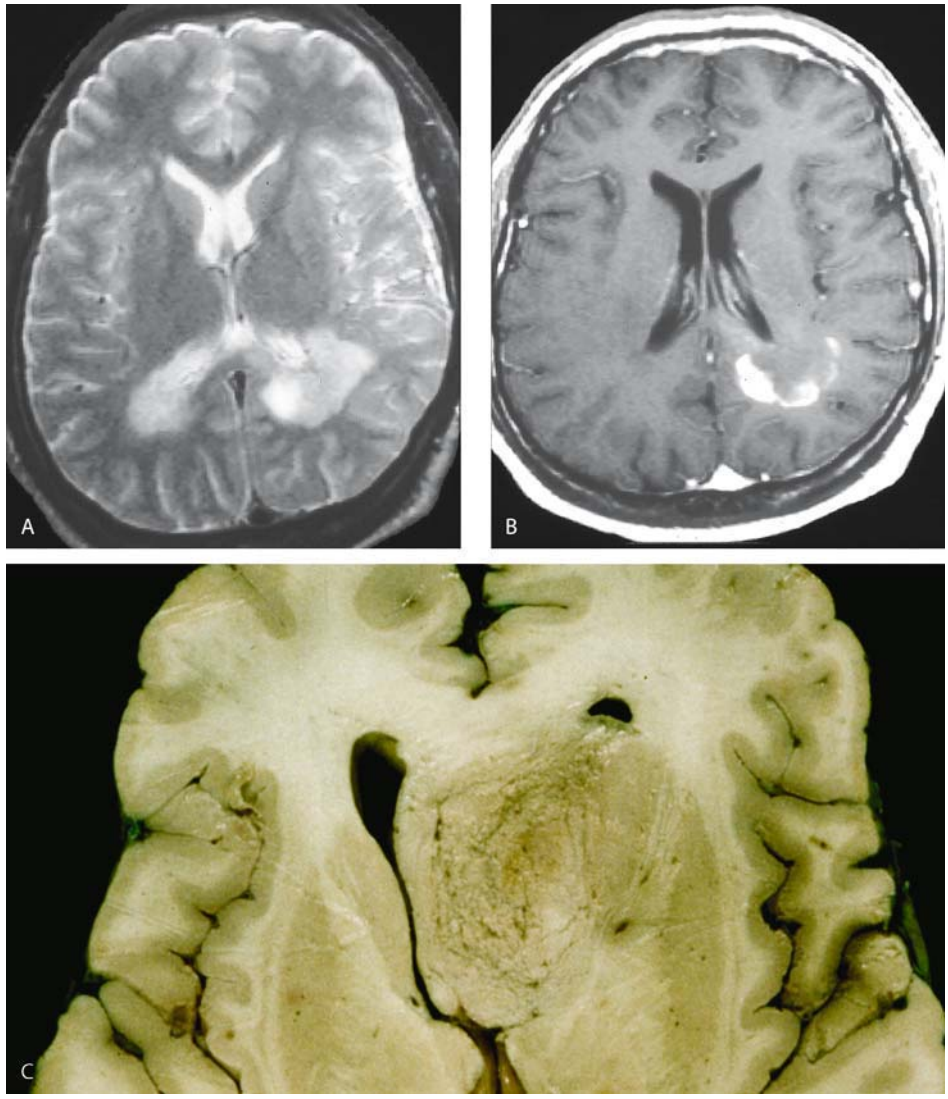

Fig. 2A–C. Anaplastic astrocytoma. **A** Axial T2-W MRI shows left hyperintense periventricular area with compression of occipital horn. **B** Axial postcontrast T1-W with enhancement incomplete ring. **C** Discernible tumor mass produces clear distinction from surrounding brain structures. This lesion infiltrates caudate nucleus, corpus callosum and lateral ventricle

Fig. 3A–C. Progression of low-grade astrocytoma to glioblastoma multiforme **(GBM).** A Baseline axial T2-weighted image shows hyperintense area without contrast enhancement. **B, C** After 2 years, glioblastoma demonstrated

Fig. 4A–C. Glioblastoma. MRI: **A** On axial T2-W the mass shows central high signal intensity due to necrosis. Note also surrounding vasogenic edema extending along the adjacent white matter (*arrows*). **B** Coronal post contrast T1-W shows central necrosis with thick and irregular ring-like enhancement. Significant mass effect. **C** Periventricular GBM in frontal lobe shows an epicenter in the white matter with granular surface and focal cystic necrosis

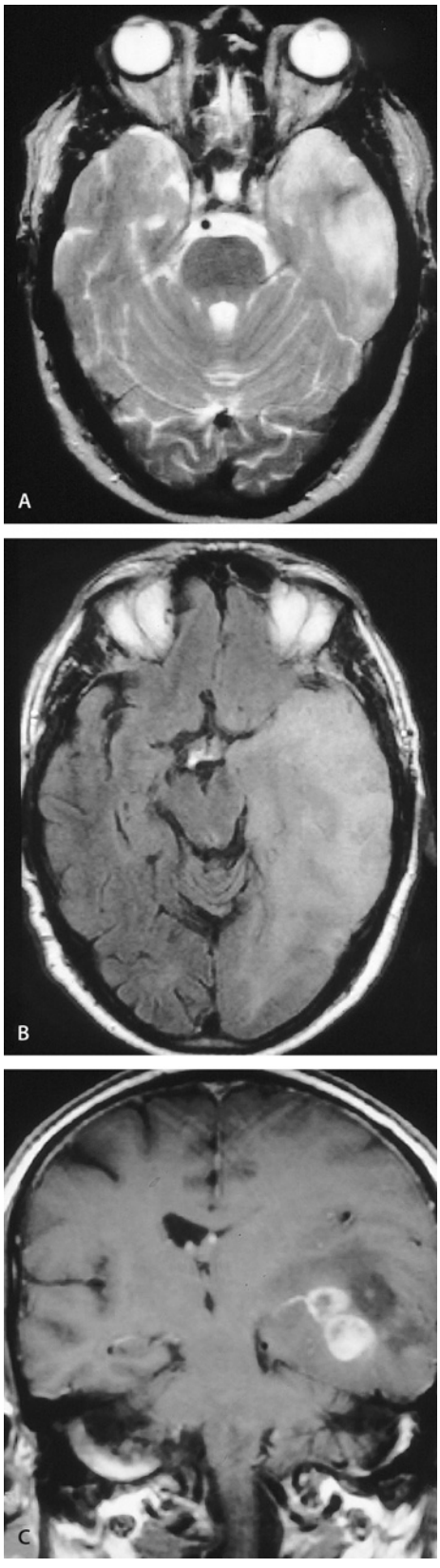

Fig. 3A–C.

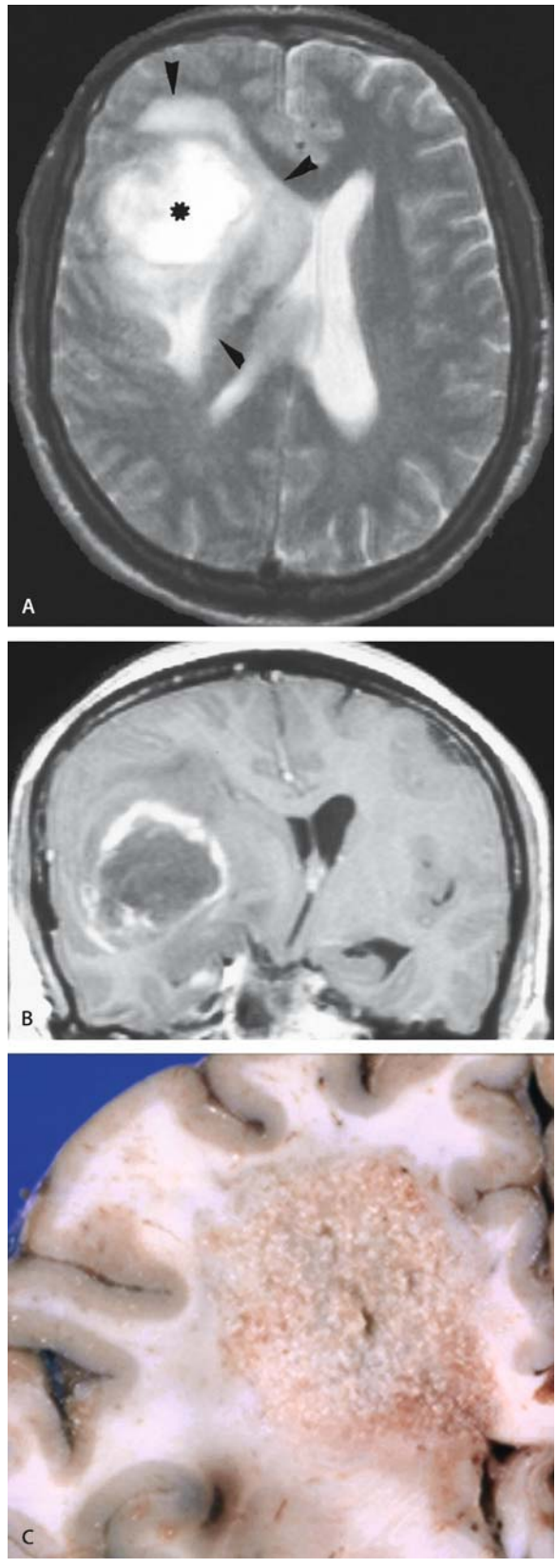

Fig. 4A–C.

Radiopathological Correlation

Glioblastomas occur most often in the cerebral hemispheres, particularly the frontotemporal and parietal regions. They are poorly delineated macroscopically, the cut surface showing a variable color with peripheral grayish tumor masses, yellowish necrosis from membrane breakdown and red and brown stipples from recent and remote hemorrhage. Central necrosis may occupy as much as 90% of the tumor mass. Macroscopic cysts, when present, contain a turbid fluid that represents liquefied necrotic tumor tissue. The lesion is usually unilateral but those in the corpus callosum can be found contralaterally (Fig. 4).

Most glioblastomas of the brain hemispheres are clearly intraparenchymal with the epicenter in the white matte (Fig. 5C); however, some are largely superficial and in contact with the leptomeninges and dura. As these latter neoplasms are frequently rich in collagen, they can be interpreted as metastatic carcinoma or as an extraaxial lesion, such a meningioma.

On CT, glioblastoma typically presents as an irregularly shaped lesion with a peripheral, ring-like zone of contrast enhancement around a dark, usually hypodense central area of necrosis (Fig. 5A, B) [12]. On T1-weighted MR images, the contrast-enhanced ring structure corresponds to the cellular and highly vascularized peripheral area of the neoplasm. Analysis whole brain sections of early untreated glioblastomas has shown that this ring structure is not the outer tumor border – infiltrating glioma cells can be easily identified within, and occasionally beyond, a 2-cm margin. In T2-weighted images, this zone is broader, less well-defined and overlaps the surrounding vasogenic edema [13].

Glioblastoma multiforme that appears as a smooth-walled cyst with a mural nodule is distinctly uncommon. A potential diagnostic pitfall is glioblastoma multiforme that manifests primarily as intraaxial hemorrhage.

Arteriovenous shunting and early filling of draining cerebral veins are commonly seen on angiographic study. Glioblastoma multiforme can be so highly vascular that it may resemble an arteriovenous malformation or a cerebral infarct with luxury perfusion.

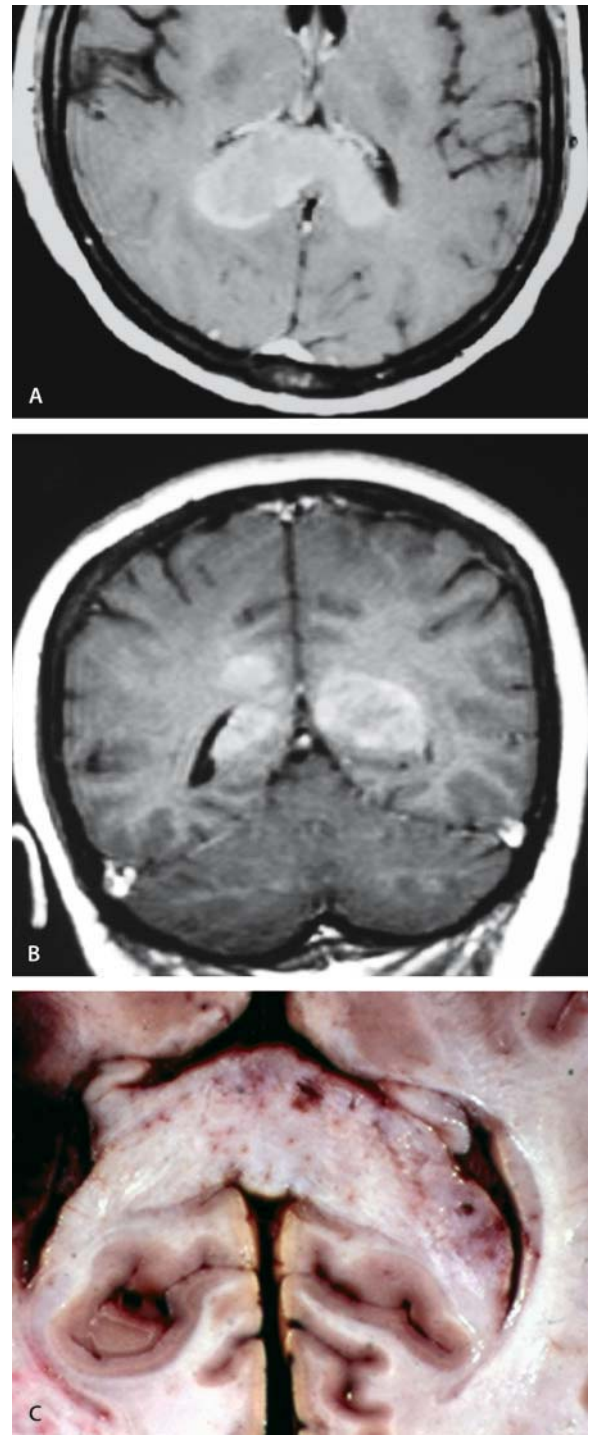

Fig. 5A–C. Glioblastoma multiforme on the splenium of corpus callosum (butterfly glioma). Axial postcontrast T1-W image (**A**) and T1 coronal shows extension of a glioblastoma multiforme through the splenium of the corpus callosum. **C** Severe enlargement of the corpus callosum and fornices. Both structures show distorted growth and granular surface

Multifocal Glioblastoma

The are three pathways that can result in multifocal glioblastoma [13, 14]:

1. primary glioblastoma spread, usually through cerebrospinal fluid pathways or through white matter tracts (Fig. 6)
2. Multiple areas of malignant degeneration occurring in a patient with diffuse, low-grade astrocytoma
3. Multiple areas of glioblastoma arising de novo in a patient with a genetic abnormality and no underlying low-grade lesion (Fig. 7).

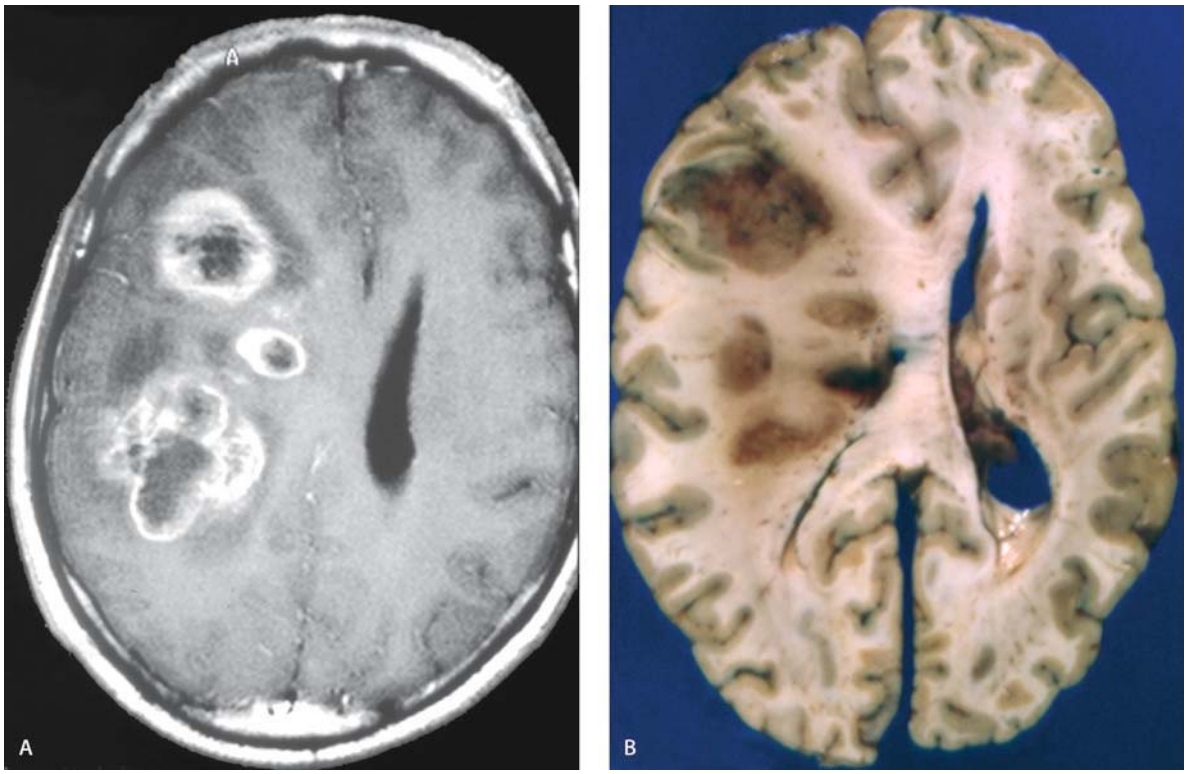

Fig. 6A, B. Multifocal glioblastoma **A** Axial postcontrast T1 MRI demonstrates multiple irregular ring enhancement lesions. **B** Axial brain section shows multiple foci of GBM in the same hemisphere. Gross features are similar in all lesions

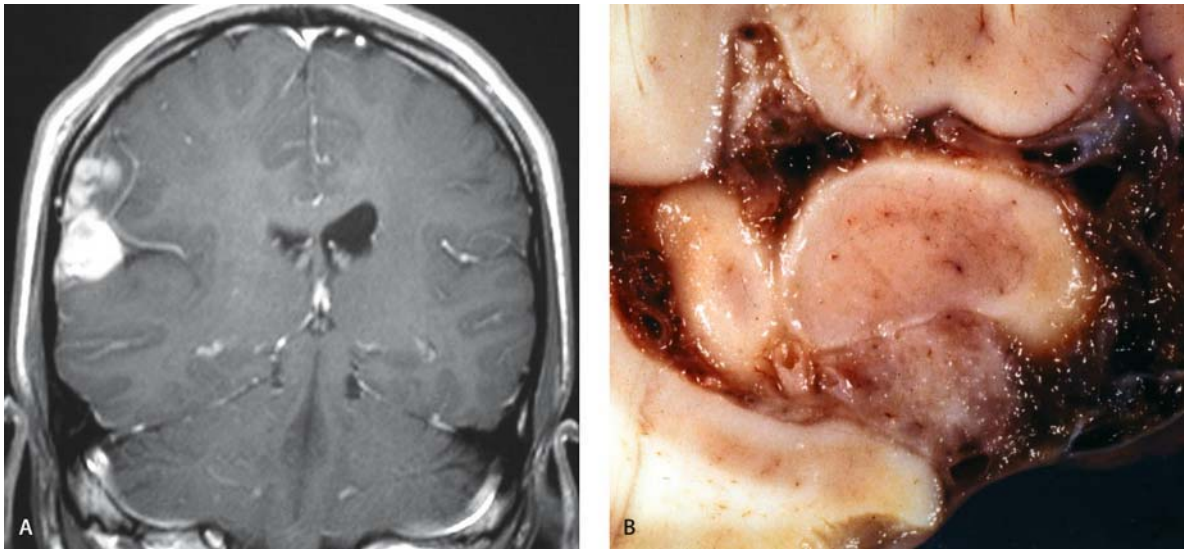

Fig. 7A, B. Patterns of glioblastoma multiforme dissemination through of the cerebrospinal fluid. **A** Coronal postcontrast T1-W image shows enhanced extra-axial mass (*arrow*). **B** Macroscopic brain section with thickened and opaque meningeal areas

Giant-Cell Glioblastoma

Giant-cell glioblastoma is a histological variant of glioblastoma with a marked predominance of bizarre, "monstrous" multinucleated giant cells and, on occasion, an abundant stromal reticulin network. They are categorized histologically as WHO grade IV and are a rare variant (less that 1% of all brain tumors) [1, 6].

Radiopathological Correlation

Giant-cell glioblastomas are distinctive because of their circumscription and firmness caused by production of tumor stroma. They are often subcortically located, in the temporal, frontal and parietal lobes. On CT and MRI, they can mimic a metastatic tumor [6, 15] (Fig. 8).

Gliosarcoma

Gliosarcoma has a sarcomatous component and accounts for approximately 2% of all glioblastomas. It is typically located in the cerebrum, and involves the temporal, frontal, parietal and occipital lobes [1, 6].

Radiopathological Correlation

The sarcomatous component produces a firm, often superficial, rather discrete mass in a lesion that may elsewhere have typical features of glioblastoma.

CT and MRI scans often show features of diffusely infiltrating glioblastoma (Fig. 9A). In cases with a predominant sarcomatous component, the tumor appears as a well-delineated hyperdense mass with homogeneous contrast enhancement, mimicking a meningioma (Fig. 9B) [16, 17]. At angiography, some gliosarcomas reveal a mixed dural and pial vascular supply [18].

Pilocytic Astrocytoma

Occurring in children and young adults, pilocytic astrocytoma is a generally well-circumscribed astrocytoma composed of a variable percentage of spongy, compact tissue [6].

These lesions are classified into WHO grade I and are the most common glioma in children [1].

The thalamus and basal ganglia are the sites of predilection in the cerebral hemispheres. Cerebral pilocytic astrocytomas are uncommon tumors that tend to affect an older group of patients than do those occurring in the cerebellum, optic chiasm or optic nerve. Cerebral hemispheres comprise 3% of cerebral gliomas [19, 20]. The right hemisphere is more commonly affected.

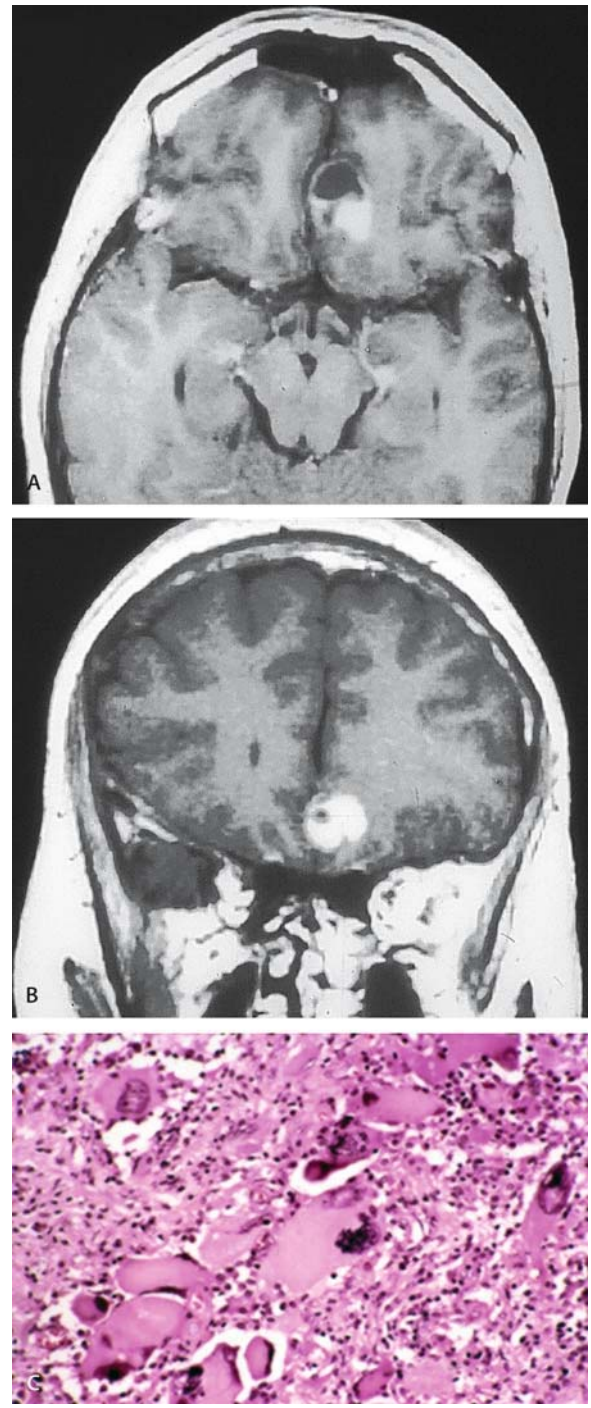

Fig. 8A–C. Giant-cell glioblastoma. Axial (**A**) and coronal (**B**) post-contrast T1-weighted MRI scans show a well-circumscribed superficial located tumor in the left gyrus rectus. **C** Typical bizarre monstrous multinucleated tumor cells are the key component in this GBM

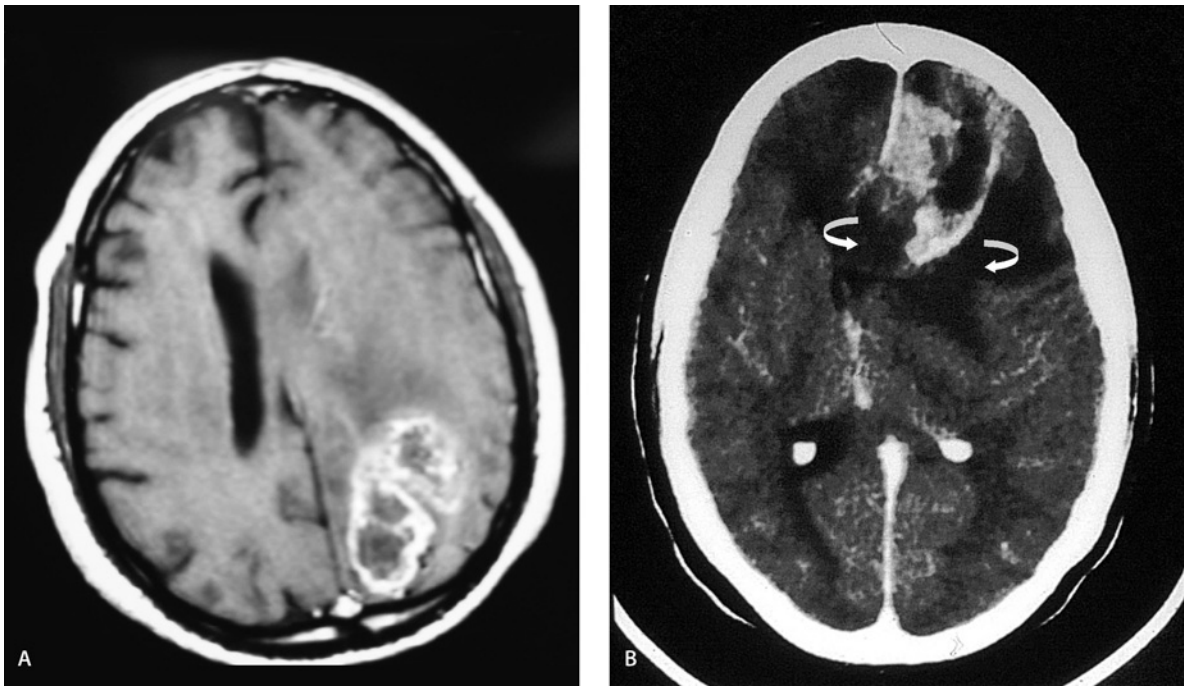

Fig. 9A, B. Gliosarcoma. **A** Axial postcontrast T1-W image. The tumor shows intense heterogeneous ring-like enhancement. **B** Axial contrast-enhanced CT in another case shows a mixed density frontal mass (the hyperdense area represents sarcomatous component). Note dural attachment (*arrow*) and peritumoral edema (*curved arrows*)

Radiopathological Correlation

Pilocytic astrocytoma is a relatively well-circumscribed lesion (Fig. 10D), often showing a heterogeneous consistency with firm or mucoid areas [21]. Focal calcification may be present. Pilocytic astrocytoma sometimes forms a mural nodule associated with cysts [22]. Invasion of the subarachnoid spaces may be evident.

CT and MR images typically show a cystic mass with an enhancing mural nodule (Fig. 10) [23–26]. Calcification occurs in 10% of cases.

Subependymal Giant Cell Astrocytoma

A discrete, large cell astrocytoma arising near the foramen is the Monro, almost always in the setting of tuberous sclerosis (TS). It is WHO grade I [1].

Clinical manifestations of SEGA usually appear during the second decade of life, but congenital examples have been encountered in premature infants. It is not uncommon to document the slow progression of an asymptomatic lesion during routine radiological screening of patients with TS.

Radiopathological Correlation

Whether solitary or bilateral, these contrast enhancing masses are solid and sharply demarcated from the underlying caudate head (Fig. 11). In their obstructive effects at the foramen, the Monro are evident on CT and MRI. The other cerebral components of cerebral tuberous sclerosis are usually evident as well [28]. These include:

1. Calcified subependymal nodules in the lateral ventricles
2. Cortical tubers with ether subjacent rarefaction or cyst formation, evident as hyperintensity on T2-WI
3. Linear abnormalities that reflect hypomyelination of the underlying white mater

Pleomorphic Xanthoastrocytoma

An astrocytic neoplasm with a relatively favorable prognosis, pleomorphic xanthoastrocytoma is typically encountered in children and young adults. It typically shows a superficial location in the cerebral hemispheres, involvement of the meninges and a pleomorphic histological appearance [2, 6]. Classified as WHO grade II, pleomorphic xanthoastrocytoma accounts for less than 1% of all astrocytic neoplasms [1].

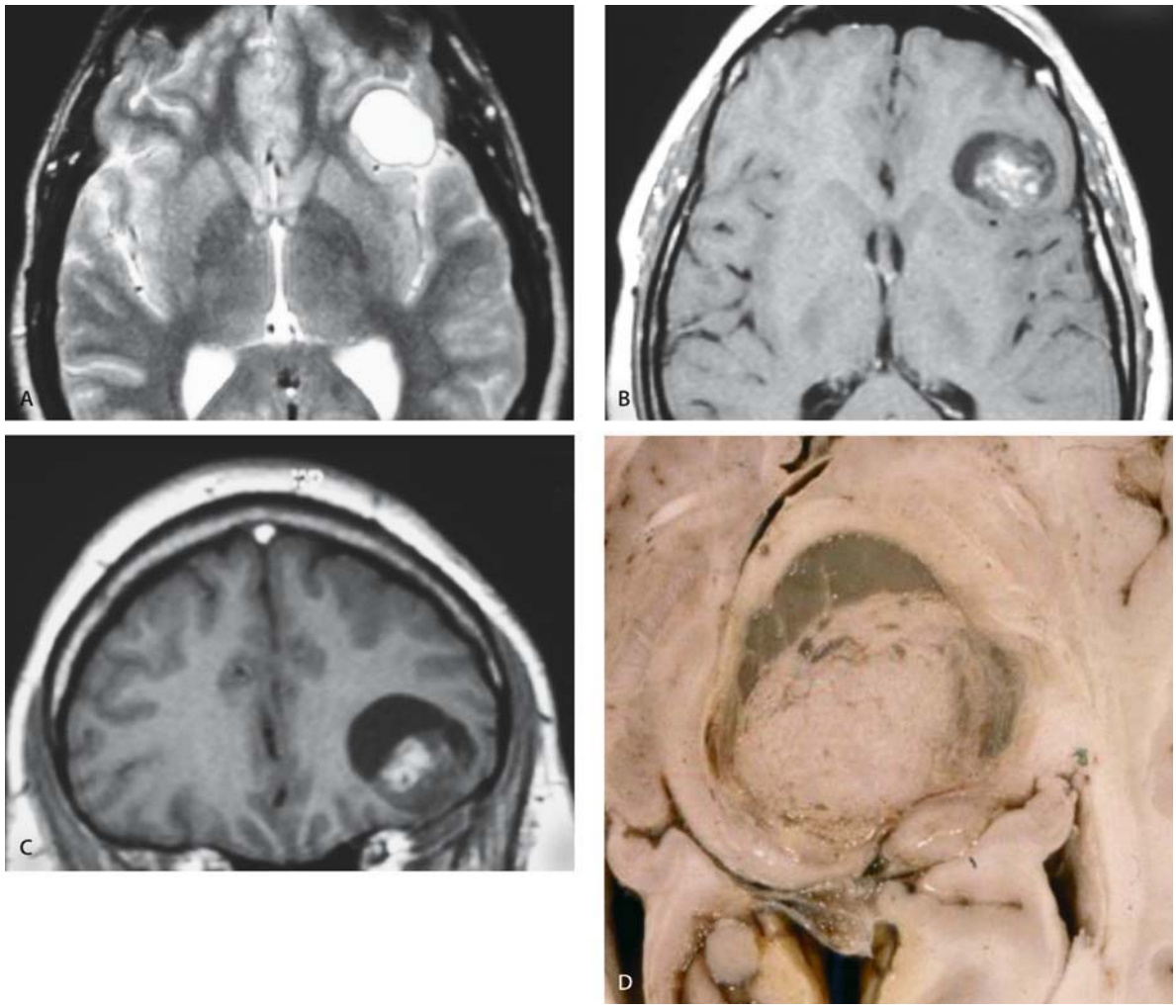

Fig. 10A–D. Pilocytic astrocytoma. Axial T2 (**A**), axial (**B**) and coronal (**C**) postcontrast T1 MRI of a pilocytic astrocytoma centered in the left frontal lobe. **D** In other patient, well-circumscribed, largely solid neoplasm with a cystic component is shown in the hypothalamic and thalamic region. Note the mural nodule (**C**, **D**)

Radiopathological Correlation

The meningocerebral type generally has a superficial location, particularly in the temporal lobe.

Pleomorphic xanthoastrocytomas are attached to the meninges and are frequently accompanied by cysts; sometime a mural nodule forms within the cyst wall. Invasion of the dura matter is exceptional.

CT and MRI scans usually outline the tumor mass and/or the cyst that is present (Fig. 12). Peripheral edema is usually not pronounced. The mural nodule enhances strongly after contrast administration [27, 29, 30].

Oligodendroglioma

Oligodendrogliomas are diffusely infiltrating tumors composed predominantly of cells morphologically resembling oligodendroglia. Histologically, oligodendroglial tumors comprise a continuous spectrum ranging from well-differentiated neoplasms to frankly malignant tumors [6]. The WHO classification system recognizes two malignant grades for oligodendroglial tumors: grade II for well-differentiated tumors, and grade III for anaplastic tumors [1].

Oligodendroglial tumors constitute only 5% of all cerebral gliomas. Although they can occur at any age, they predominate in adults, with a peak incidence in the fifth and sixth decades. The most common signs are epileptic seizures and headache.

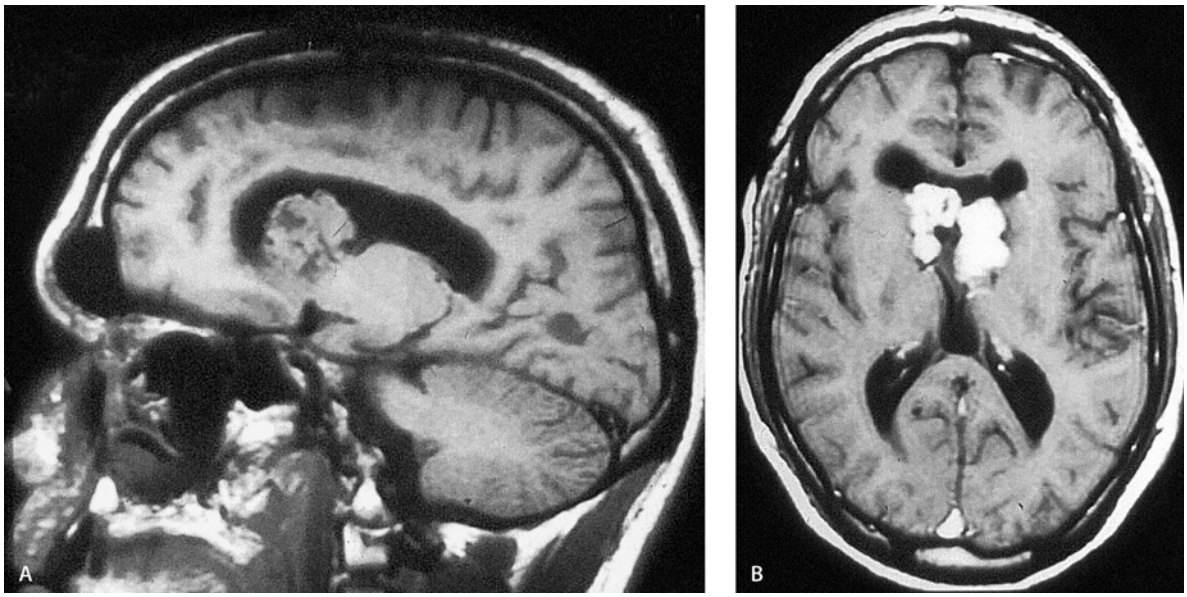

Fig. 11A, B. Subependymal giant-cell astrocytoma in a patient with tuberous sclerosis. **A** Sagittal T1-weigthed image shows a heterogeneous mass in the foramen of Monro. **B** Axial postcontrast T1-weighted image with intense enhancement

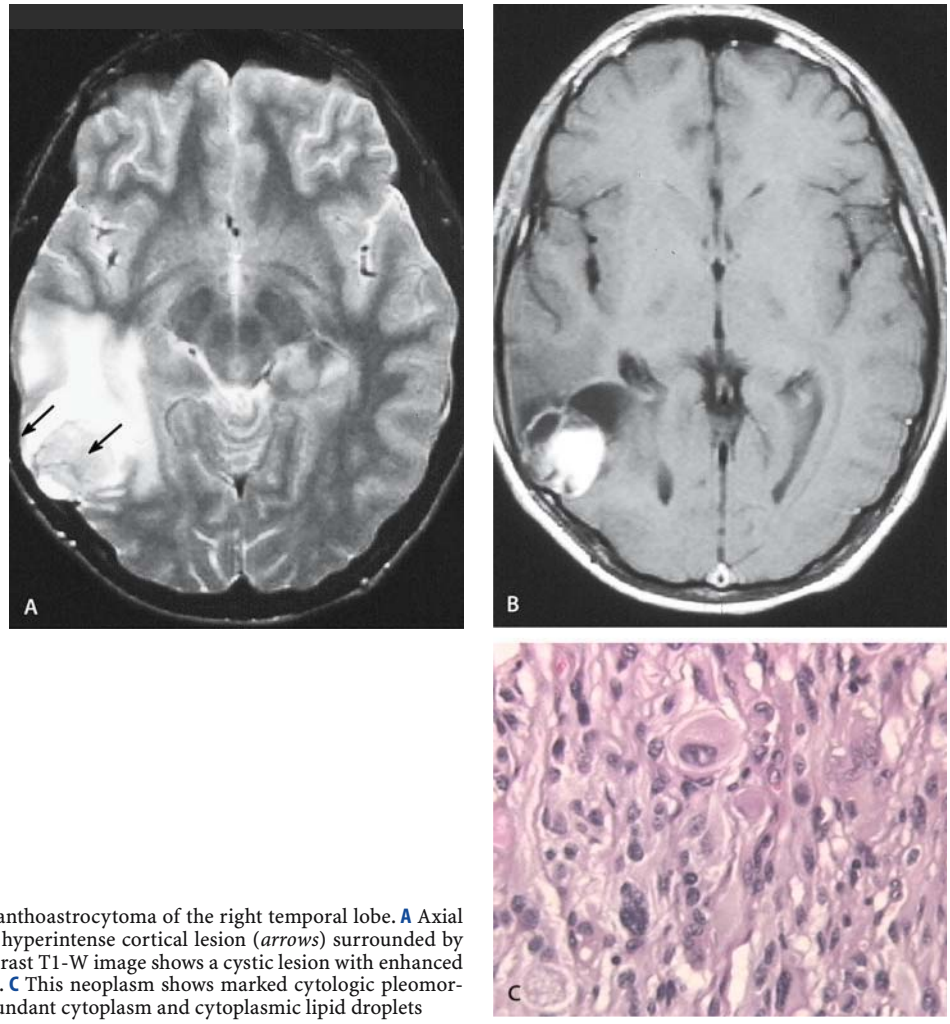

Fig. 12A–C. Pleomorphic xanthoastrocytoma of the right temporal lobe. **A** Axial T2-weighted image shows hyperintense cortical lesion (*arrows*) surrounded by edema. **B** Coronal postcontrast T1-W image shows a cystic lesion with enhanced peripheral nodule (*arrow*). **C** This neoplasm shows marked cytologic pleomorphism. Many cells have abundant cytoplasm and cytoplasmic lipid droplets

Radiopathological Correlation

Macroscopically, they appear as well-defined soft, grayish pink masses. Cyst degeneration and necrosis can occur in large lesions. Typically, oligodendrogliomas affect the cerebral cortex and subcortical white matter of the cerebral frontotemporal regions. Infiltration of the adjacent leptomeninges is common. Anaplastic oligodendrogliomas may demonstrate areas of tumor necrosis.

On CT, the tumors are usually hypo- or isodense in comparison to the normal gray matter. Calcification is common (Fig. 13). Mild contrast enhancement may be seen in a fraction of cases. Peripheral edema is usually mild or not seen. Calvarial erosion occurs in about 17% of cases [31].

MRI studies typically demonstrate a hypointense lesion in the T1-weighted images and a hyperintense lesion in T2. The tumors are well-delineated and show little perifocal edema. However, some may demonstrate heterogeneous images of variable intensities due to intratumoral hemorrhage and/or areas of cystic degeneration. Although enhancement is more frequently identified with MR imaging than with CT, it is usually modest. Anaplastic oligodendrogliomas may show nonhomogeneous patterns and contrast enhancement is usual.

Mixed Gliomas

Mixed gliomas are tumors composed of a conspicuous mixture of two or more distinct neoplasia counterparts of the normal macroglial cell types. By far the most common mixed gliomas are oligoastrocytomas [6].

Oligoastrocytomas are tumors composed of mixture of two different neoplastic cell types morphologically resembling the tumor cells in oligodendroglioma or low-grade diffuse astrocytoma (WHO grade II). The oligodendroglial and astroglial components may be either diffusely intermingled or separated into distinct areas.

Mixed gliomas correspond histologically to WHO grade II and the anaplastic types to grade III [1].

Radiopathological Correlation

Generally, mixed gliomas cannot be differentiated from other WHO grade II or III gliomas by their gross appearance.

On imaging studies, they demonstrate no special features that would provide reliable clues to distinguish them from other gliomas (Fig. 14). In the series published by Shaw et al. [32], calcifications were demonstrated in 14% of these tumors. About half of the oligoastrocytomas evaluated by CT and MRI showed contrast enhancement.

Ependymoma

Ependymoma is a tumor predominantly composed of neoplastic ependymal cells, with preferential manifestation in children and young adults. Anaplastic ependymoma is a variant with histological evidence of advanced anaplasia, including nuclear atypia, marked mitotic activity, high cellular, microvascular proliferation and necrosis [6].

Histologically, ependymoma are low-grade and correspond to WHO grade II. Anaplastic ependymomas are classified as WHO grade III [1]. Ependymomas account for 2%–4% of supratentorial tumors. The age distribution is slightly lower for supratentorial than for infratentorial location and males are affected slightly more frequently than females.

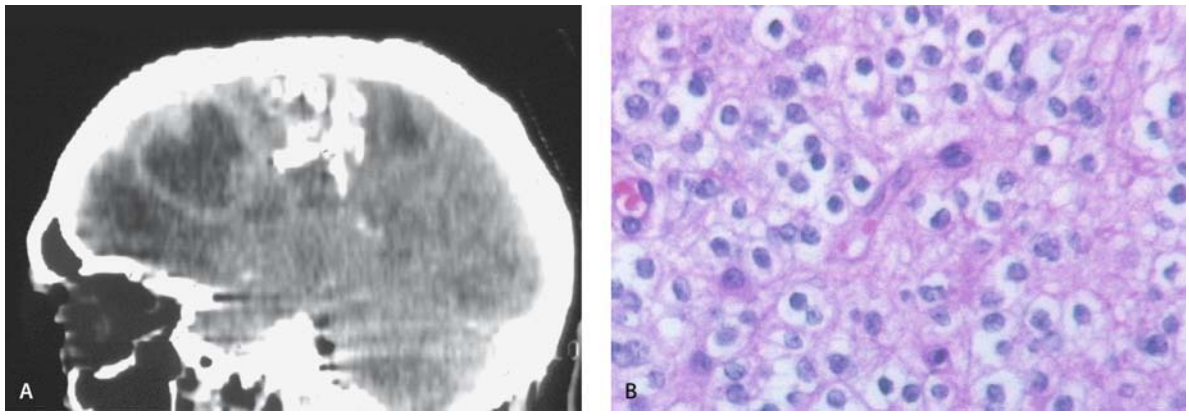

Fig. 13A, B. Oligodendroglioma. **A** CECT sagittal reformation shows frontal tumor with calcification. **B** Classic picture with diffuse pattern of regular round cells with clear perinuclear halo

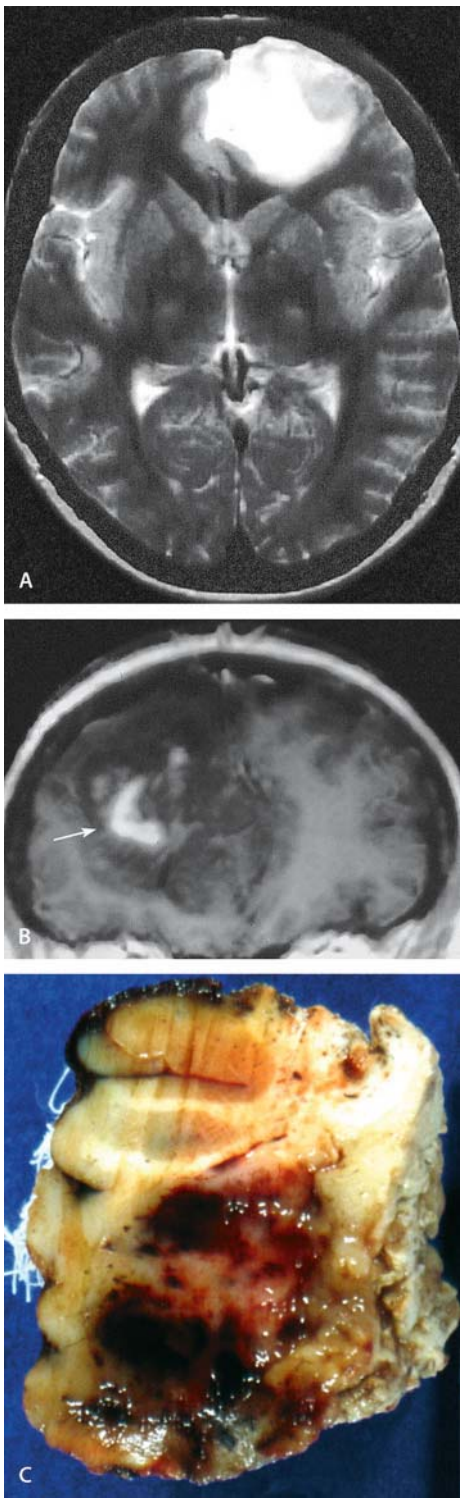

Fig. 14A–C. Oligoastrocytoma. **A** Axial T2-weighted MR scan shows a frontal hyperintense well-demarcated lesion with mild perifocal edema. **B** Coronal postcontrast T1-W image demonstrates a focus of enhancement (*arrow*). **C** Gross appearance of the frontal lobe shows an oligoastrocytoma with recent hemorrhagic component after incomplete removal of tumor

The white matter of the frontal and parietal lobes is most commonly involved, some parts of the cerebral hemispheres can be affected. Cerebrospinal fluid dissemination occurs frequently, especially with recurrence of the tumor.

Radiopathological Correlation

Supratentorial ependymomas intrude upon the ventricular system, but also enlarge centrifugally into the surrounding brain where they present to the surgeon as freshly gray and, most importantly, relatively discrete masses. Since the epicenter in the ventricular zone may not be apparent, the diagnosis may be not suspected when approached laterally. Ependymomas are soft, gray masses with or without cysts, necrotic foci or hemorrhage.

On CT and MRI, these tumors have a variable, heterogeneous appearance [33–35]. They are usually large (>4 cm) and well-demarcated. Cyst formation or necrosis is typical (70%–80%), as is calcification (50%). Hemorrhage into the lesion occurs occasionally [36]. Moderate to intense contrast enhancement is the rule (Fig. 15). CT scan demonstrates a heterogeneously hypodense to isodense mass. Increased density can be seen if hemorrhage has occurred, and anaplastic lesions often have higher attenuation. MRI reveals a heterogeneous lesion that is hypointense to isointense on T1-weighted images and hyperintense on T2. Gadolinium often shows a rather well-circumscribed lesion with varying intensity of contrast enhancement. MRI is particularly useful in determining the relationship to surrounding structures and invasion along cerebrospinal spaces [35, 36].

Subependymoma

Subependymoma is a well-differentiated, nodular, and highly fibrillar ependymal tumor generally situated within a ventricle. It is WHO grade I.

Subependymoma are most often encountered as an incidental finding. The lateral ventricle near the caudate nucleus (40%–75%) and the floor of the fourth ventricle (30%–60%) are the most common locations. Like ependymomas, occasional examples occur near the surface of the brain.. Based on critical location and size, hydrocephalus is the most common presentation [37].

Radiopathological Correlation

As lobulated, flat-based tumors, subependymoma are firmly attached to their site of origin. Although basically soft than solid, the texture of long-standing lesion may be modified by calcification, hemorrhage, or cyst

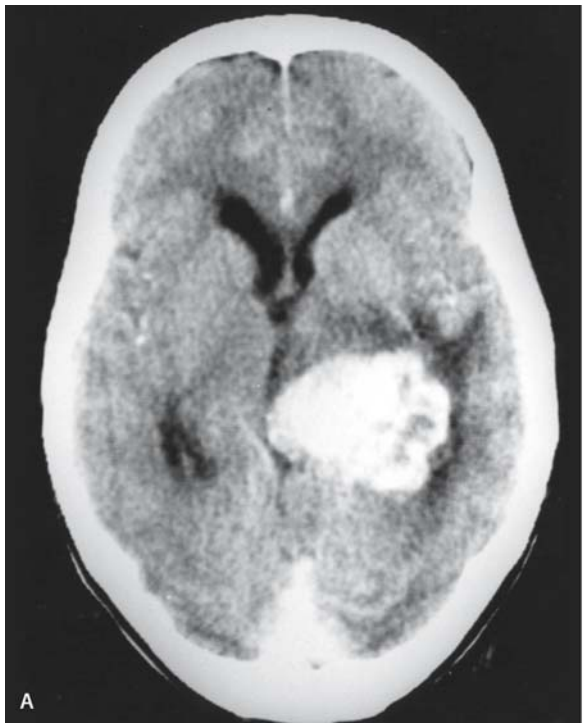

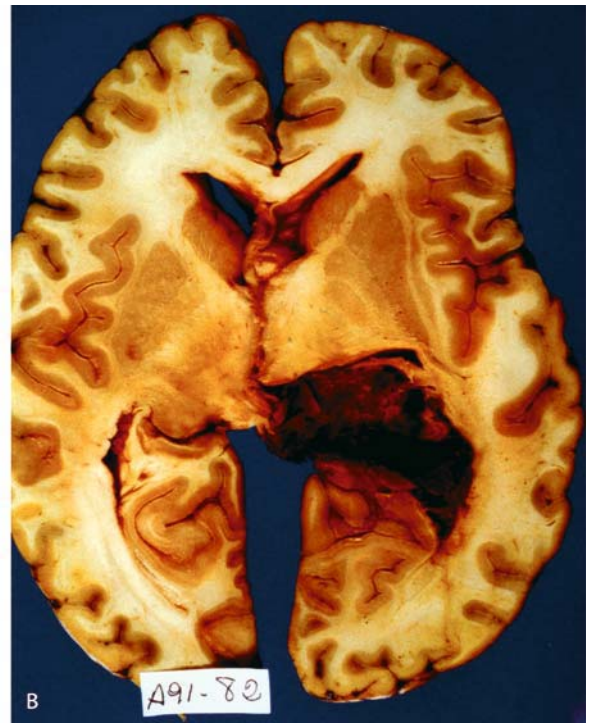

Fig. 15A, B. Ependymoma supratentorial. **A** Axial contrast-enhanced CT demonstrates homogeneous enhancing mass in the atrium of the right lateral ventricle. **B** In this axial section of the brain, the right temporal horn is occupied by a well-defined hemorrhagic granular tumor

formation. The tumor is characterized by small group of ependymal cells in a rather dense, delicately fibrillar stroma. Calcifications, hemorrhage and/or microvascular proliferation may be formed.

Radiological findings show lateral ventricle subependymoma on CT [38], which vary in density, but are more often hypodense, and usually do not enhance. Calcifications are seen in less 10% of cases. On MRI, they are typically hypointense to gray matter on T1-WI and hyperintense on T2-WI (Fig. 16). As with CT, they seldom demonstrate enhancement and are thus readily distinguished from other lateral ventricle tumors, which typically do enhance. Subependymoma do not demonstrate paraventricular extension.

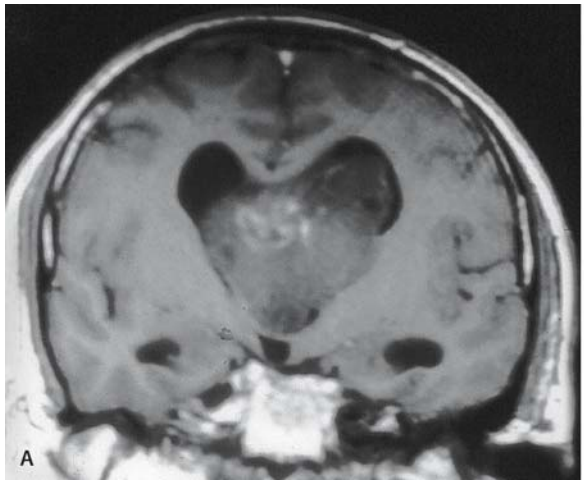

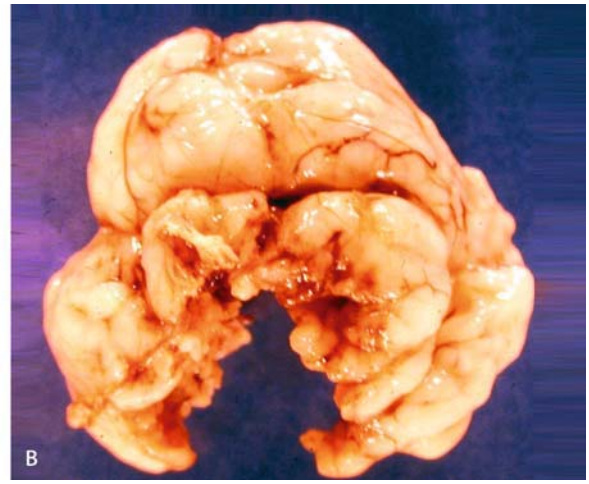

Fig. 16A, B. Lateral ventricle subependymoma. **A** Coronal postgadolinium T1-weighted image. Lack of contrast enhancement discerns this neoplasm from others in the same location. **B** Macroscopic appearance after surgical removal shows nodular surface

Choroid Plexus Tumors

Choroid tumors are papillary neoplasms of the cerebral ventricles derived from choroid plexus epithelium. Choroid plexus papilloma is classified as WHO grade I, whereas choroid plexus carcinoma is histologically malignant (WHO grade III) [1, 6].

Although choroid plexus tumors account for only 0.4%–0.6% of all brain tumors, they represent 2%–4% of those that occur in children and 10%–20% of those manifesting in the 1st year of life. Around 80% of lateral ventricle tumors present in patients under 20 years old. Choroid plexus tumors tend to block cerebrospinal pathways.

Radiopathological Correlation

Choroid plexus papillomas are circumscribed, cauliflower-like masses that adhere to the ventricular wall, but are usually well-delineated in relation to the brain tissue. Choroid plexus carcinomas are invasive tumors that may appear solid, hemorrhagic and necrotic [36].

Choroid plexus papillomas are well-circumscribed, lobulated intraventricular masses. Ventriculomegaly or effacement of the lateral ventricles is often present. The majority are isodense to hyperdense, with about a quarter of the lesion being hypodense, on CT images. They are brightly enhancing tumors that may have calcifications [39].

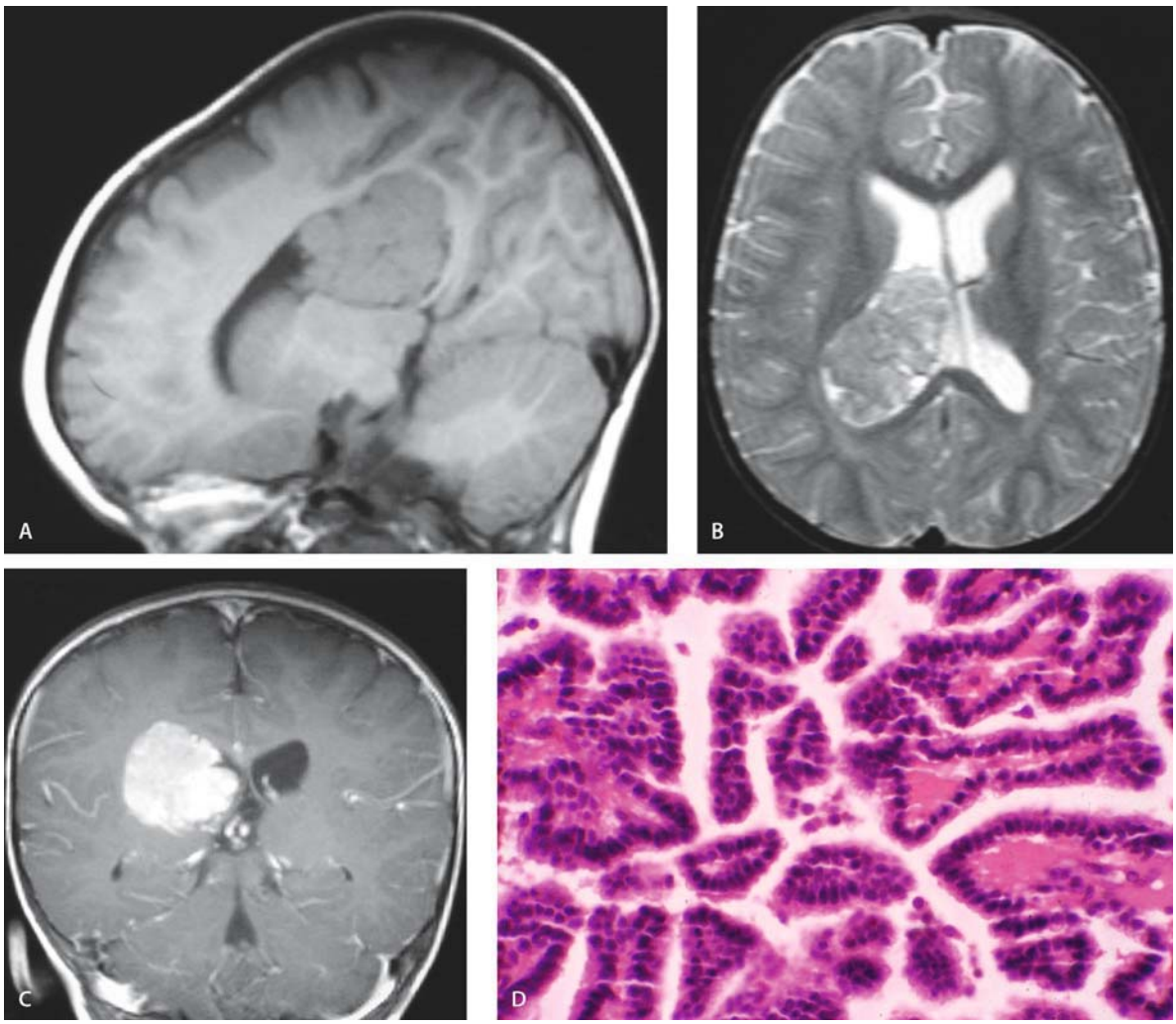

Fig. 17A–D. Choroid plexus papilloma. **A** Sagittal T1-weighted image shows a large, almost isointense intraventricular mass. **B** Axial T2-weighted image shows heterogeneous, high signal intensity mass, causing hydrocephalus. **C** Coronal T2 postcontrast image shows a markedly enhanced intraventricular mass. **D** Obvious papillary architecture is found. The layer of cuboidal cells without atypia is characteristic

On MRI (Fig. 17), choroid plexus papillomas are isointense to hypointense to the brain tissue and hyperintense to the cerebrospinal fluid in T1-weighted images. There are areas of signal void, suggesting increased regional blood flow or calcifications. On T2-weighted images, 60% are hyperintense to the parenchyma. Gadolinium enhancement is uniform [40, 41].

Angiography may demonstrate tumor blush. Lateral ventricular lesions are associated with enlarged choroid arteries [41].

Choroid plexus carcinomas often grow through the ventricular wall and invade the surrounding brain. They are of varied density on precontrast scan and enhance nonhomogeneously on postcontrast CT. Cysts, calcifications and hemorrhages are frequent.

On MRI they show mixed signal intensities on T1-weighted images because of the presence of cysts and hemorrhage. Irregular enhancement is noted after gadolinium.

Choroid plexus carcinomas have a marked propensity to metastasize through the cerebrospinal pathways, sometimes forming large subarachnoid masses [42] (Fig. 18).

Neuroepithelial Tumors of Uncertain Origin

Astroblastoma

Astroblastoma is a glial neoplasm characterized by a typical perivascular pattern of GFAP-positive astrocytic cells with broad, nontapering processes radiating towards central blood vessels [6]. Astroblastoma occurs most frequently in young adults, occasionally in children and rarely in infants. A case of congenital astroblastoma has been reported [43].

Radiopathological Correlation

The cerebral hemispheres are most often affected. Macroscopically, they are usually well-circumscribed solid masses with a homogeneous cut surface, although large examples may show both cyst formation and necrosis [36].

On CT and MRI, they are often enhancing, well-defined lesions (Fig. 19).

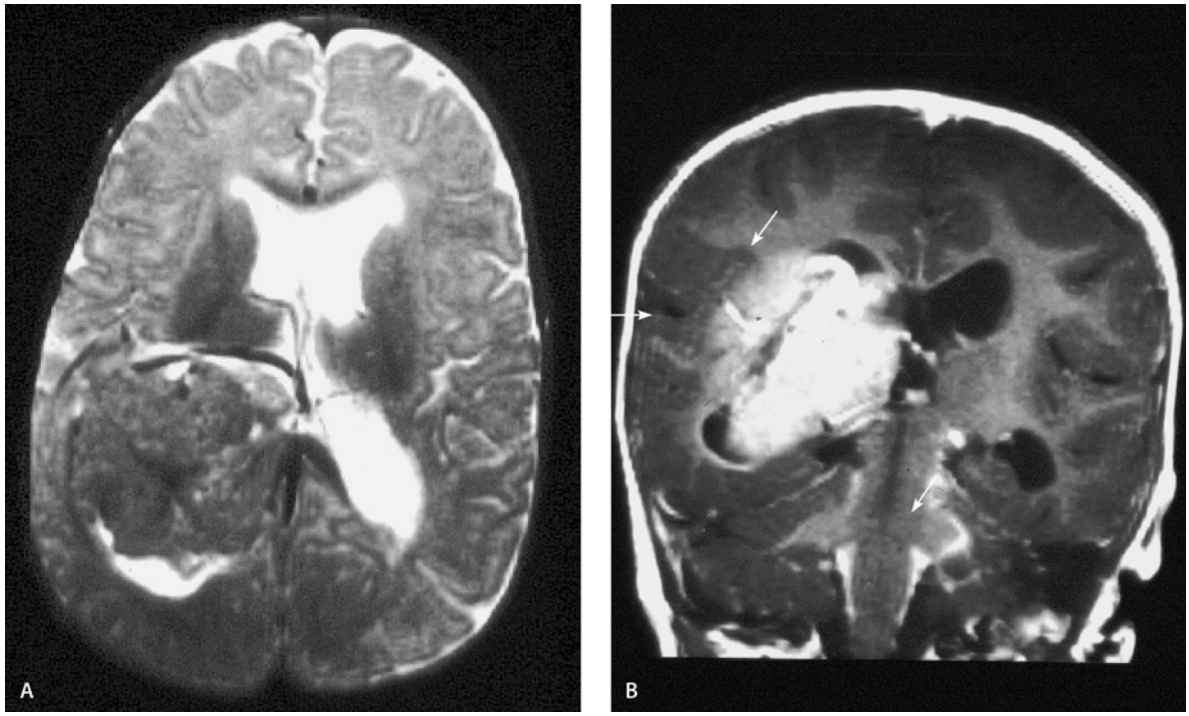

Fig. 18A, B. Congenital choroid plexus carcinoma. Axial T2-weighted (**A**) and coronal T1 postgadolinium images (**B**) of a choroid plexus carcinoma involves the trigone and right lateral ventricle. Note the hydrocephalus, a frequent finding among patients with choroid plexus tumors. This tumor tends to invade adjacent brain (*arrowheads*) and subarachnoid space (*arrow*) more readily, as seen in this case (**B**)

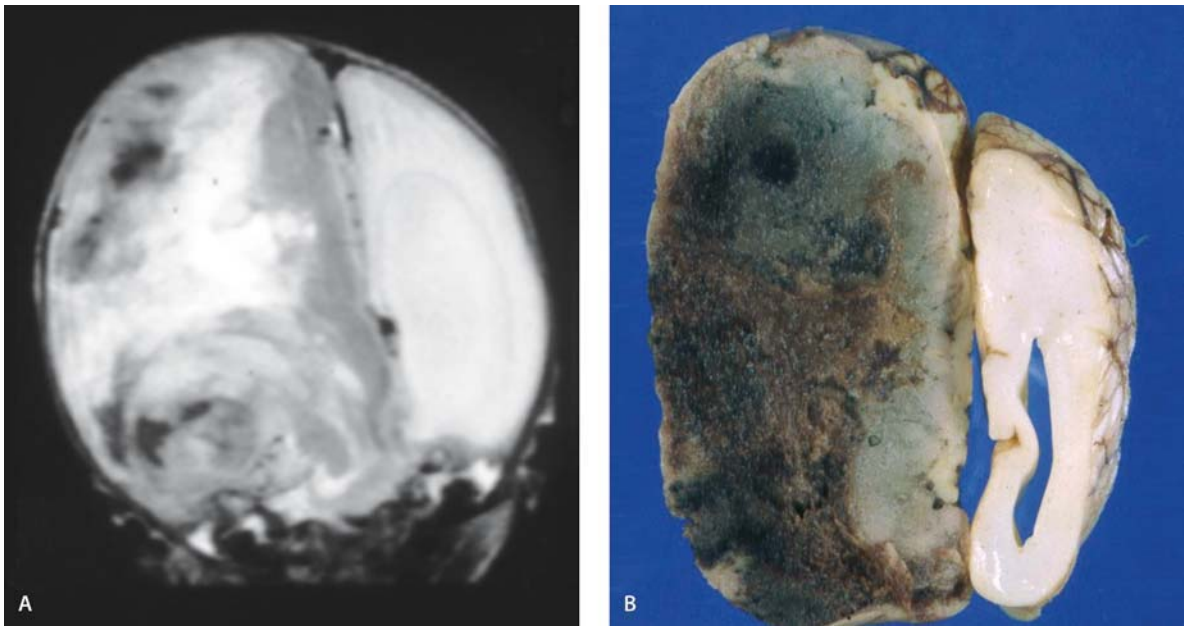

Fig. 19A, B. Astroblastoma. **A** Coronal T2-weighted MRI shows a large mixed-intensity tumoral mass with necrotic focus. **B** Extensive, well-circumscribed extensive hemispheric tumor with hemorrhagic component is a rare case of congenital tumor in a 35-weeksgestation newborn

Gliomatosis Cerebri

Diffuse glial tumors infiltrating the brain extensively so as to involve more than one lobe, gliomatosis cerebri are frequently bilateral and often extend to infratentorial structures and even the spinal cord [6].

Gliomatosis cerebri are malignant lesions, corresponding to grade III or IV in the WHO classification [1]. The term "gliomatosis cerebri" was originally coined by Nevin in 1938 [44] to describe infiltration by glial cells of extensive areas of the brain without formation of an obvious tumor mass.

Radiopathological Correlation

The most commonly affected areas, as defined by postmortem studies and images are: cerebrum (76%), mesencephalon (52%), pons (52%), and thalamus (43%). When the lesion involves the cerebral hemispheres, the centrum semioval is always affected, whereas the cortex is infiltrated in only 19% of such cases.

Macroscopically, two types of gliomatosis cerebri have been distinguished. Type I is the classic lesion, in which there is diffuse neoplastic growth and enlargement of involved existing structures, without the formation of a circumscribed mass. Type II gliomatosis, which may develop from type I, is associated with the presence of an obvious neoplastic mass, usually a malignant glioma [45].

On both on CT and MRI [46, 47], the pattern is infiltrative, with enlargement but not destruction of the involved structure. The gyri are swollen and flattened and the sulci are obliterated. On CT study, the lesion appears as poorly defined areas of low density [45]. In the T1-weighted images, MRI shows hypointense areas, whereas proton-density images and T2 reveal the full extension of the tumor with hyperintensity (Fig. 20). Enhancement is rare but has been seen in type II gliomatosis. We believe that ante-mortem diagnosis is possible by means of the correlation between the radiological findings and brain biopsy

Hemangioblastoma Supratentorial

Supratentorial hemangioblastomas are rare, although less than originally believed, owing to their earlier confusion with vascular meningiomas [1]. They probably represent about 5% of all cases and occur in a variety of locations, including the pituitary stalk, optic nerve and third and fourth ventricles. Proportions are hemispheric and superficial, and may show dural attachment or lie entirely within the leptomeninges. Both posterior fossa and supratentorial hemangioblastomas may be multiple at the time of presentation, especially in the context of von Hippel–Lindau disease (VHL).

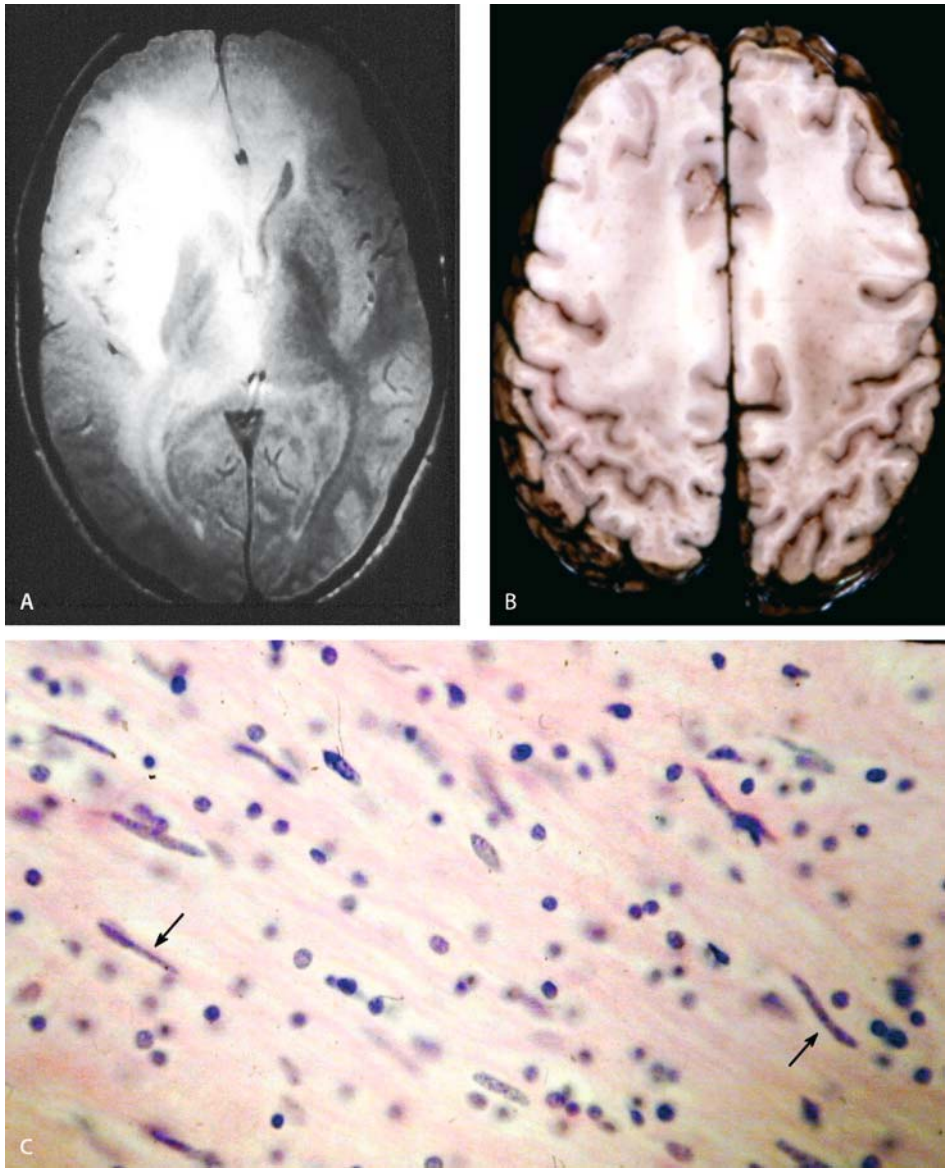

Fig. 20A–C. Gliomatosis cerebri. **A** Axial T2-weighted MRI scan shows extensive infiltration of the white and gray matter in both hemispheres and corpus callosum with obliterated sulci. **B** Axial section of the brain shows diffuse enlargement in the greater part of both centra semiovales. Note widened flattened circumvolutions and obliterated sulci in the left frontal lobe. **C** White matter, in centrum semiovale, shows diffuse infiltration by neoplastic spindle-shape astrocytes

Radiopathological Correlation

Macroscopic features are hemangioblastomas that are well-circumscribed red-brown tumors that may be totally intraparenchymal, partly extraparenchymal or entirely extra-axial. The intraparenchymal tumors usually have a superficial margin at the pial surface, and this is often covered by ecstatic and tortuous superficial blood vessels. Supratentorial hemangioblastomas sometimes have a dural attachment and grossly recable margins, especially when they are predominantly extraparenchymal. Intraventricular examples may appear macroscopically similar to ependymomas. Something over two-thirds of hemangioblastomas at any site take the form of a large cystic lesion with a well-defined, often quite small mural nodule. The cyst usually contains yellow or brown proteinaceous fluid, which coagulates at room temperature. Angiography has been the traditional radiological investigation of choice for intracranial hemangioblastoma (Fig. 21C) and remains an important diagnostic procedure despite the advent of CT and MRI [48]. In addition to establishing the blood supply and

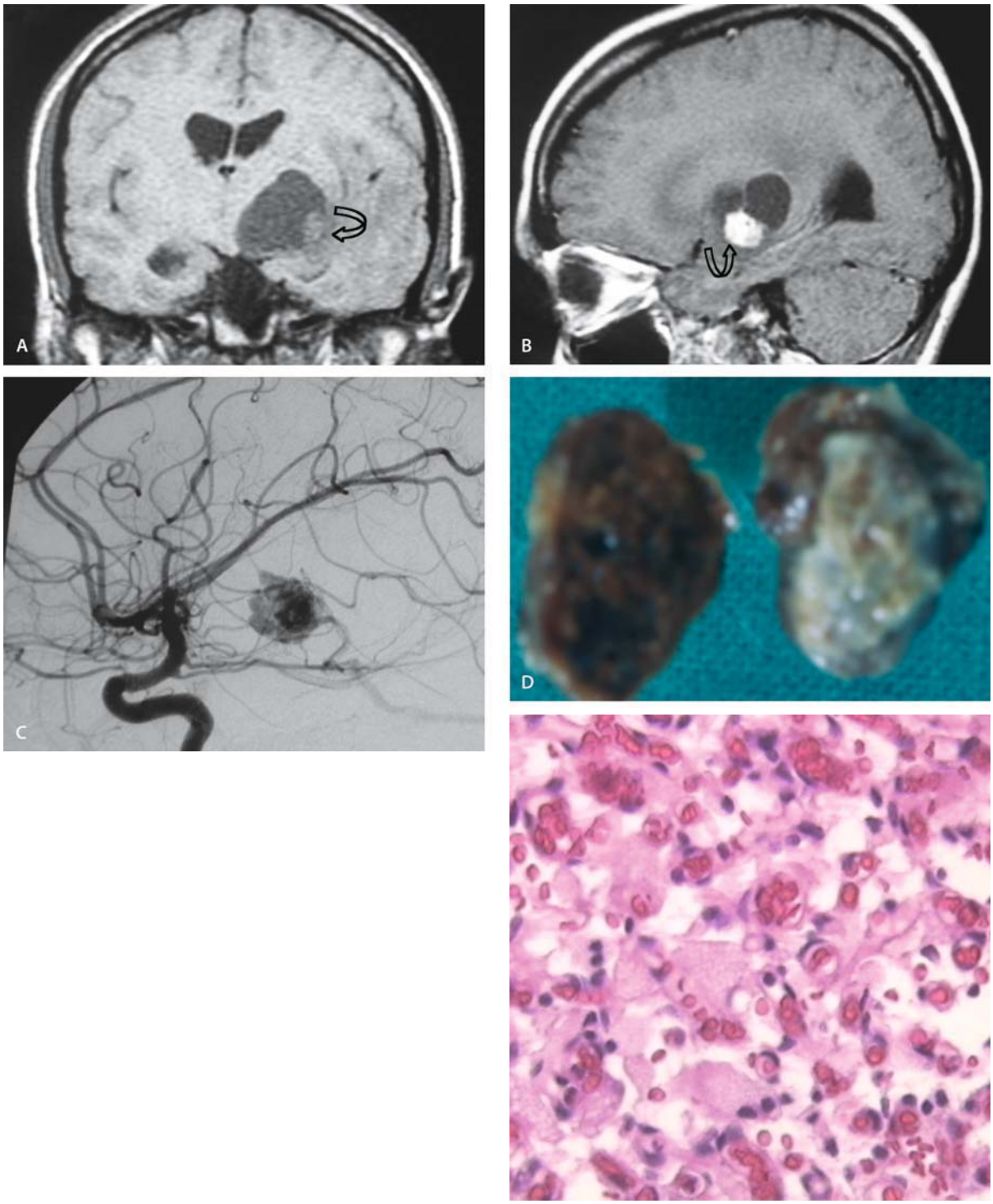

Fig. 21A–E. Supratentorial hemangioblastoma. Coronal T1-weighted image (**A**) and sagittal T1 image after contrast administration show a cystic lesion and an isointense mural nodule (*curved arrow*). Strong enhancement of the mural nodule (**B**). Carotid angiography (**C**) shows a vascular mural nodule. **D** The removed nodule shows in the cutting a cystic and hemorrhagic surface while it is nodular externally. **E** A network of capillary channels with interstitial clear cells are characteristic features

vascular drainage of the tumor, angiography is a sensitive method of locating noncystic examples and allows detection of other unsuspected tumors overlooked by localized scans. For cystic tumors, CT allows precise definition at the cystic cavity and is often used in combination with angiography. Solid tumors and mural nodules are isodense with brain and not well seen in nonenhancement scans, but they show uniform, intense enhancement with intravenous contrast media. MRI again provides a good definition of cystic tumors, which are visible as well-defined low-signal areas, slightly hyperintense to CSF on T2-W. However, gadolinium administration is essential to identify to mural nodules of cystic lesions and to define the extent of solid tumors (Fig. 19). MRI also allow visualization of the large abnormal vessels feeding and draining the tumors, which show as flow void on T2-W [49].

Chordoid Glioma of the Third Ventricle

The lesion presents in adults with the generic symptoms attributable to the obstructing third ventricle mass. Females are more frequently affected.

Radiopathological Correlation

Macroscopic features are the solid lobulated lesion that often distends the third ventricle and adheres to the wall. The lesion has a sharp interface with surrounding brain parenchyma. Its substance consists of ribbons, cords, and lobule of uniform, epithelial-like cells in a faintly basophilic, mucinous matrix [50]

Radiological Features

The lesions are remarkably similar from case to case, all are discrete, smooth-contoured, contrast-enhancing, third-ventricle masses that obstruct CSF flow and produce hydrocephalus [51].

Neuronal and Mixed Neural-Glial Tumors

Gangliocytoma and Ganglioglioma

Tumors are composed of neoplastic, mature ganglion cells, either alone (gangliocytoma) or in combination with neoplastic glial cells (ganglioglioma) [6]. Gangliocytoma is classified into WHO grade I, while ganglioglioma may be grade I or II [1]. These two types represent 1.3% of all brain tumors. Any age can be affected, but 80% occur in individuals under 30 years old.

Patients typically present with seizures or focal neurological signs. These tumors preferentially occur in the temporal lobe, followed by the frontal and parietal lobes.

Radiopathological Correlation

Macroscopically, gangliocytomas and gangliogliomas are solid or cystic tumors that are not usually accompanied by mass effects. Calcification may be present. Hemorrhage and necrosis are rare.

CT shows a well-circumscribed mass, often peripherally located in the cerebral hemispheres. The lesion may be solid or cystic. The tumor is isodense or hypodense and may show calcifications. Surrounding edema is only occasionally noted, and hemorrhage is rarely identified. Contrast is variable and usually of moderate intensity. Scalloping of the calvaria may be seen adjacent to superficially located tumors [52, 53].

On MRI the most common appearance is a well-delineated temporal or frontal lobe mass that is hypointense in T1- and hyperintense in T2-weighted images (Fig. 22). Enhancement varies in intensity from weak to marked, and may be solid, at the rim or nodular [54].

Desmoplastic Infantile Ganglioglioma

Desmoplastic astrocytoma is a clinicopathological entity (WHO grade I), characterized by large tumors that involve the superficial cortex and occur in infants, with a generally good prognosis following surgery [5].

Desmoplastic gangliogliomas are rare supratentorial neuroepithelial neoplasms that present in early infancy, between 1 and 24 months of age (mean, 6.3 months). They invariably arise in the supratentorial region and affect more than one lobe, preferentially the frontal and parietal, followed by the temporal.

The symptoms and signs are of short duration and include increasing head circumference and tense, bulging fontanelles.

Radiopathological Correlation

Macroscopically these tumors are large, measuring up to 13 cm in diameter, and have deep uni- or multiloculated cysts filled with clear or xanthochromic fluid. The solid superficial portion is primarily extracerebral, involving the leptomeninges; the superficial cortex is commonly attached to the dura [55].

Plain skull films show sutural diastasis with or without erosion of the internal table adjacent to the tumor. On CT, the lesion is a large, well-defined cystic region, similar to cerebrospinal fluid, with a solid isodense or slightly hyperdense superficial portion, which shows contrast enhancement (Fig. 23). T1-weighted MR images characteristically show a hypointense cystic mass

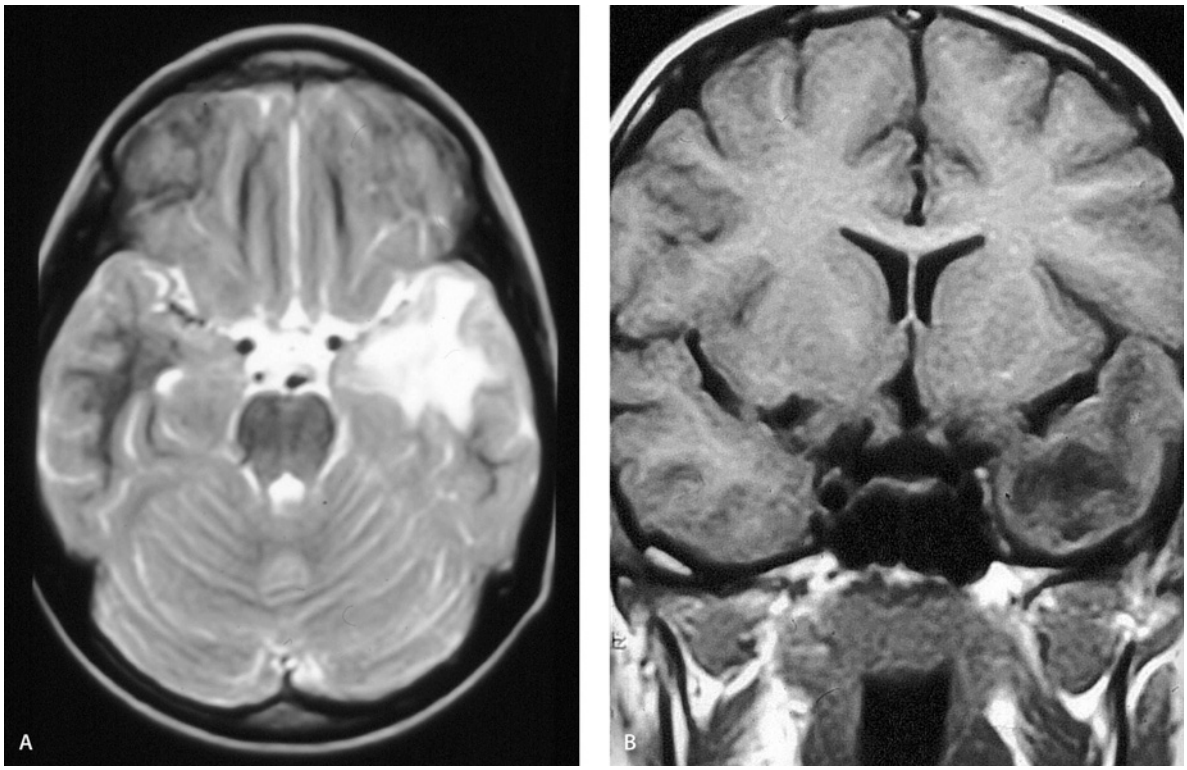

Fig. 22A, B. Ganglioglioma. **A** Axial T2-weighted image demonstrates hyperintense left temporal lobe mass. **B** Coronal T1-weghted image shows low-intensity area

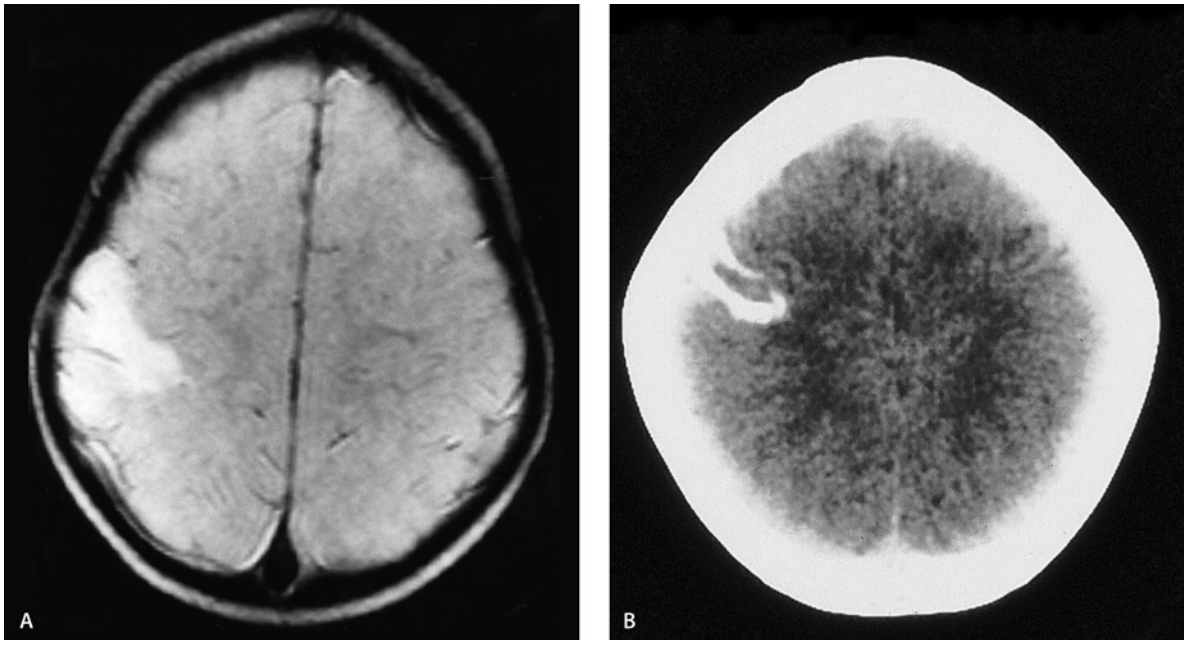

Fig. 23A, B. Dysembryoplastic neuroepithelial tumor. **A** Axial T2-weighted MR image shows a well-demarcated hypersignal. The cortical topography of the lesion, which looks like microgyri, can be seen. **B** CT in the same patient demonstrates gyral calcifications and involvement of the overlying calvaria

with a peripheral solid component that enhances with gadolinium. The solid portion is heterogeneous in T2-weighted images.

Dysembryoplastic Neuroepithelial Tumor

Dysembryoplastic neuroepithelial tumors (WHO grade I) are benign, usually supratentorial mixed glial neuronal neoplasms, characterized by multinodular architecture and a predominantly intracortical location. They may be associated with cortical dysplasia [4, 56].

A large majority of dysembryoplastic neuroepithelial tumors that are identified during surgery for epilepsy are located in the temporal lobe and preferentially involve the mesial structure [57]. However, they may develop in any part of the supratentorial cortex.

Radiopathological Correlation

The gross appearance may reflect the complex histological architecture of the lesion. The most typical feature is the viscous consistency of the ganglioneural component. The affected cortex is often expanded and, although the tumor is predominantly intracortical, the subcortical white matter may also be affected.

On imaging, the cortical topography of the lesion is an important criterion for differentiating between these tumors and gliosis. On CT, definition of the overlying calvaria is often seen, and this finding supports the diagnosis of dysembryoplastic neuroepithelial tumors. Calcifications are often present (Fig. 24B).

Hypointense on the T1-weighted and hyperintense on the T2-weighted MR images, these tumors can resemble macrogyria (Fig. 24A). True cyst formation is seen in a minority of cases. About one-third show contrast enhancement on CT or MRI, which often appears as multiple rings [58, 59].

Central Neurocytoma

A WHO grade I neoplasm composed of uniform round cells with neuronal differentiation, central neurocytoma is typically located in the lateral ventricles, in the region of the foramen of Monro [3, 60]. These tumors affect mainly young adults, and have a favorable prognosis. The incidence of central neurocytoma is estimated at 0.2%–0.5% of all intracranial tumors.

The clinical history is short and the majority of patients present with symptoms of intracranial hypertension.

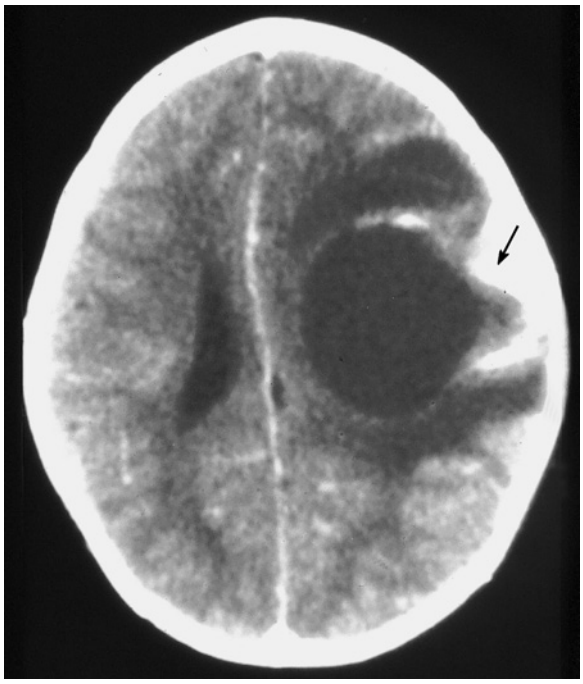

Fig. 24. Desmoplastic infantile ganglioglioma. CT after contrast administration. Cystic and solid (*arrow*) components

Radiopathological Correlation

Macroscopically, central neurocytoma is a soft, well-circumscribed neoplasm that often contains flecks of calcification and occasional hemorrhage.

On CT, the majority are visualized as well-circumscribed nonhomogeneous masses, which are isodense or slightly hyperdense to the parenchyma. Calcifications (52%) and cystic areas (67%) are often seen (Fig. 25A). Contrast enhancement and associated hydrocephalus are present [61, 62].

On MRI, the T1- and T2-weighted images show an essentially isointense lesion with nonhomogeneous regions reflecting areas of calcification and cyst formation. Areas of hypointensity in T1-W images are probably related to focal calcification, and areas of hyperintensity on T2-W to areas of cystic necrosis. Tumor enhancement is moderate to strong after gadolinium administration [61, 62] (Fig. 25B).

Cerebral angiography demonstrates a faint tumor blush persisting into the late venous phase [63].

Cerebral Neuroblastoma

The neuroblastoma is a another small blue cell tumor of presumed neuronal linage that occurs as a tumor of children and young adults: approximately half are diagnosed in the first 5 years of life.

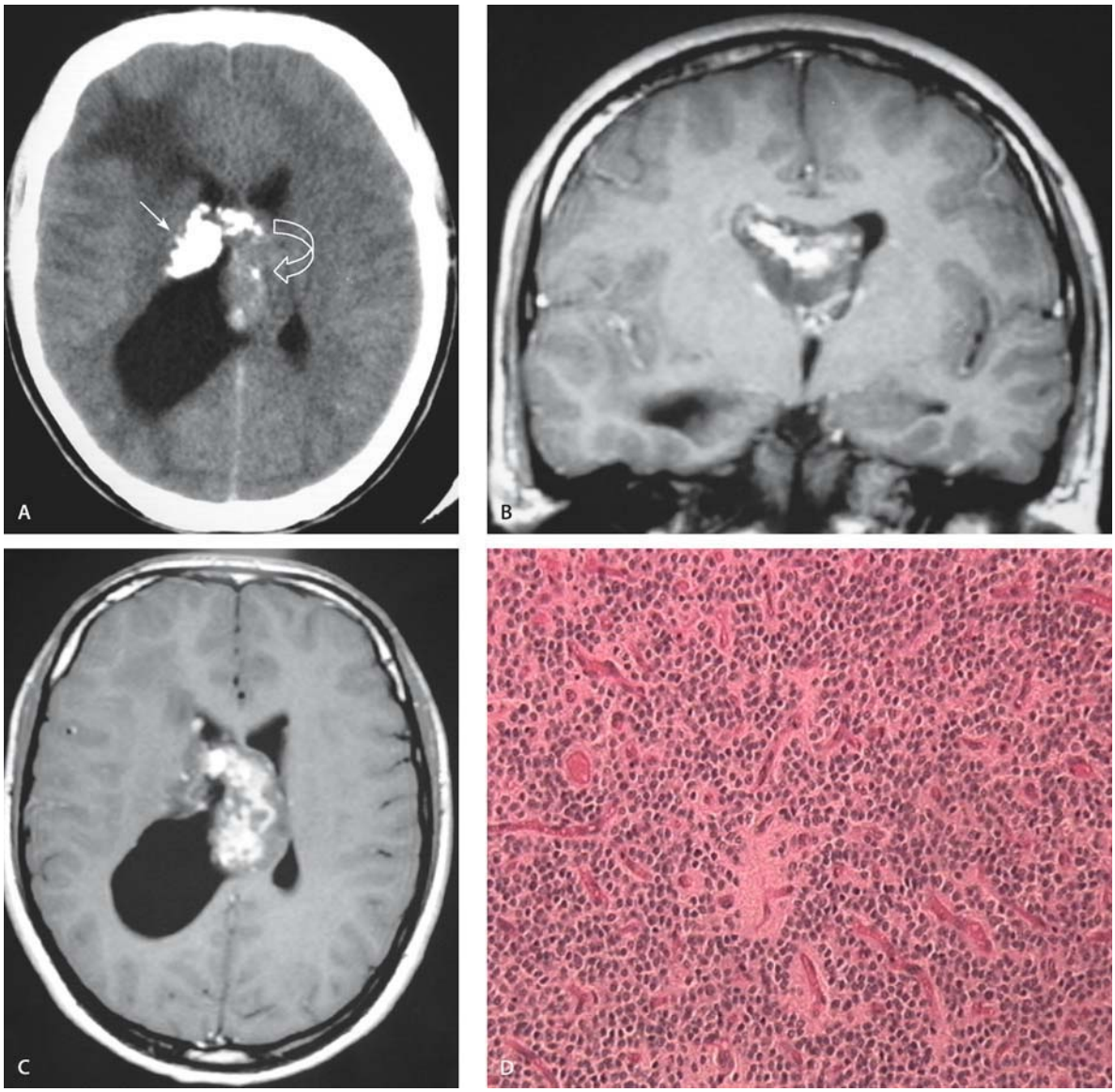

Fig. 25A–D. Central neurocytoma. **A** CT shows mixed calcified (*arrow*) and isodense (*curved arrow*) intraventricular mass. No symmetrical hydrocephalus. Coronal (**B**) and axial (**C**) postcontrast T1-weighted MR image shows a large enhancing tumor occupying the frontal horns of both lateral ventricles with obstruction of the foramen of Monro. **D** A sheet of cells with uniform, round nuclei which have fibrillary cytoplasm

Radiopathological Correlation

The macroscopic appearance shows the neuroblastoma growing as expansile masses, within the brain, typically with gross circumscribed, pushing borders and often has attained a large size (several centimeters in diameter) by time of diagnosis. The tumors tend to be firm and are particularly superficial and desmoplastic. Multilobulation and cyst formation are common, the cyst often as large than the tumor itself. Widespread dissemination along the CSF pathways is a common finding at autopsy.

The unenhanced CT appearance is that of an inhomogeneous mass with hypodense regions due to necrosis and cyst formation and hyperdense regions due to calcification. A large amount of mass effect and edema is commonly present. Inhomogeneous contrast enhancement is typically seen. Dissemination through the subarachnoid space and ventricular system can be seen as foci of abnormal contrast enhancement within such spaces.

The lesions are inhomogeneous on T2-W MRI due to the presence of necrosis and hypointense regions of hemorrhage and calcification. Contrast enhanced MRI

is more sensitive than CT for determining tumor extent, including subarachnoid and meningeal spread.

Supratentorial Primitive Neuroectodermal Tumor

Supratentorial primitive neuroectodermal tumor (WHO grade IV) is an embryonal tumor composed of undifferentiated or poorly differentiated neuroepithelial cells, which have a capacity for divergent differentiation along neuronal astrocytic, ependymal, vascular or melanotic lines. Primitive neuroectodermal tumors are uncommon in the supratentorial compartment [64].

Radiopathological Correlation

The parenchymal tumors are massive growths with or without cysts or hemorrhage. The demarcation between tumor and brain may range from indistinct to clear-cut. They are soft, unless they contain a prominent desmoplastic component.

Imaging typically reveals a large mass deep in the cerebral white matter. Necrosis or cyst formation is seen in 30%–60%, with calcifications in 50%–70%. Hemorrhage is always noted and may be solid, heterogeneous or ring-like, depending on the degree of cystic or necrotic changes (Fig. 26). The lesions are iso- to hyperdense on CT. Surrounding edema is not usually extensive [65, 66].

Lymphomas

Malignant lymphomas of the CNS include: 1) primary CNS lymphomas (PCNSL), defined as extranodal malignant lymphomas arising in the CNS in the absence of obvious lymphoma outside the CNS at the time of diagnosis, 2) secondary involvement of the CNS in systemic lymphoma.

The current annual incidence [61] in immunocompetent patients is 0.3 new cases per 100,000 person–years. In AIDS patients, the incidence of 4.7 per 1000 person–years is about 3,600-fold higher than in the general population. Primary CNS lymphoma is the second most common (following toxoplasmosis) CNS mass lesion in adult AIDS patients and is the most common mass lesion in pediatric AIDS patients. Secondary CNS involvement by systemic lymphoma occurred in approximately 25% of cases before the advent of effective chemotherapy.

Epstein-Barr virus is implicated in the pathogenesis of PCNSL in all immunocompromised patients and 15%–20% of immunocompetent patients.

About 60% of primary CNS lymphoma involve the supratentorial space. The cerebral white matter of the frontal lobes is the most common site for CNS lymphoma, and in the temporal, parietal and occipital lobes in decreasing order of frequency. Approximately 2%–50% are multiple. Secondary meningeal spread is seen in 30%–40% of primary lymphomas. One of the most characteristic features of CNSL is its tendency to spread through the ependyma, the meninges, or both.

Peak incidence is seen in the sixth and seventh decades in immunocompetent patients and in the fourth decade in immunocompromised patients.

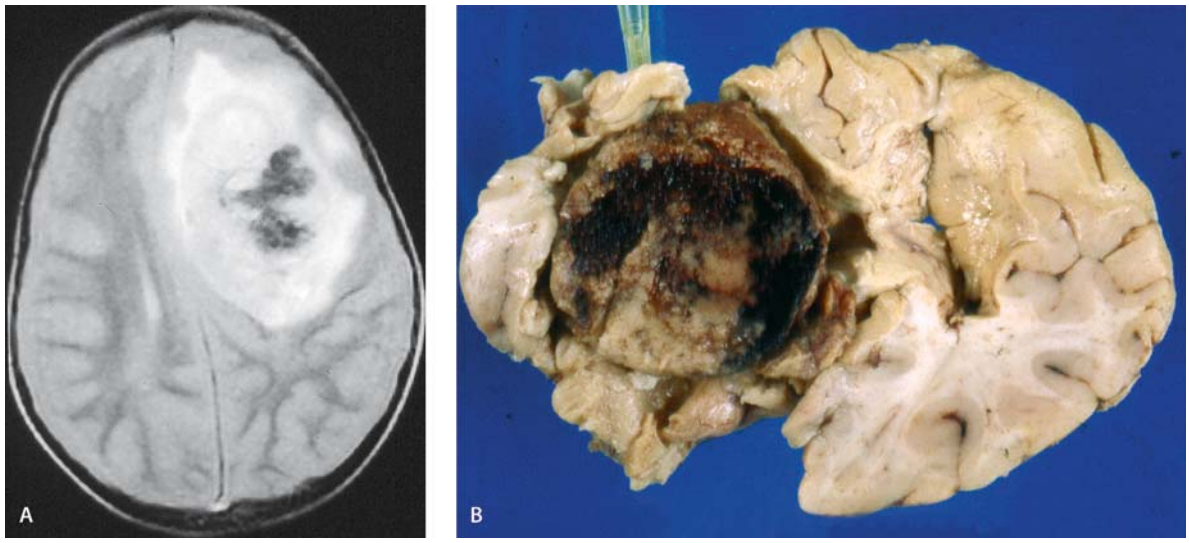

Fig. 26A, B. Primitive neuroectodermal tumor. **A** Axial T2-weighted image MR scan shows heterogeneous left frontal mass with hemorrhage (low-signal areas). **B** A sharply circumscribed and soft tumor in the left frontal lobe occurred in a 6-year-old girl. Terminal intratumoral hemorrhage can be seen

PCNSL present as space-occupying lesions causing raised intracranial pressure, focal neurological deficit or epilepsy.

Radiopathological Correlation

Macroscopically, primary lymphomas appear as simple or multiple masses in the cerebral hemispheres. While they are often deep-seated and adjacent to the ventricular system, superficial tumors are also encountered. The tumors manifest as grayish-tan to pink homogeneous, circumscribed nodular masses with a firm to friable consistency and a granular surface. The lesion is frequently surrounded by edema. Demarcation from the surrounding parenchyma is variable. Some tumors appear well-delineated, as in metastasis. When a diffuse border and architectural effacement is present, the lesions resemble gliomas. It is impossible to grossly determine the extent of the tumor. Focal necrosis is present in AIDS patients.

The infiltrated meninges appear thick, and subependymal intraventricular spread may manifest as areas of irregularity and softening.

Non-AIDS lymphomas appear as hyperdense masses on nonenhanced CT examination because of the cellularity of the lesion, with little associated edema. In AIDS-related CNS lymphoma, the lesion may be hyperdense or hypodense on noncontrast CT. Hypodensity is often related to the high degree of necrosis present in AIDS-related lymphomas. The hypodense lesions often have hyperdense rims where there is less necrosis. Hemorrhage in this lesion is uncommonly seen on CT. Calcification is rare. There is usually a variable degree of mass effect and edema.

Postcontrast CT demonstrates dense enhancement, which is homogeneous in non-AIDS lymphoma but may be homogeneous (Fig. 27), heterogeneous, or show ring enhancement in AIDS-related lymphoma. This again may be related to the greater frequency of necrosis in the latter. Periventricular enhancement suggests subependymal spread and is often a valuable clue in the radiographic diagnosis of CNS lymphoma [67, 68].

The dense cellularity of lymphoma renders these lesions isointense or hypointense to the parenchyma in all MRI sequences. These signal characteristics strongly suggest the diagnosis in the appropriate clinical setting. Administration of gadolinium results in solid or ring-like enhancement. Ring enhancement is more frequently associated with necrotic lesions. Nonenhancing PCNSL has been thought to be extremely rare (Fig. 28) [69, 70].

The recent use of T1 brain SPECT has made it possible to differentiate between these tumors and infec-

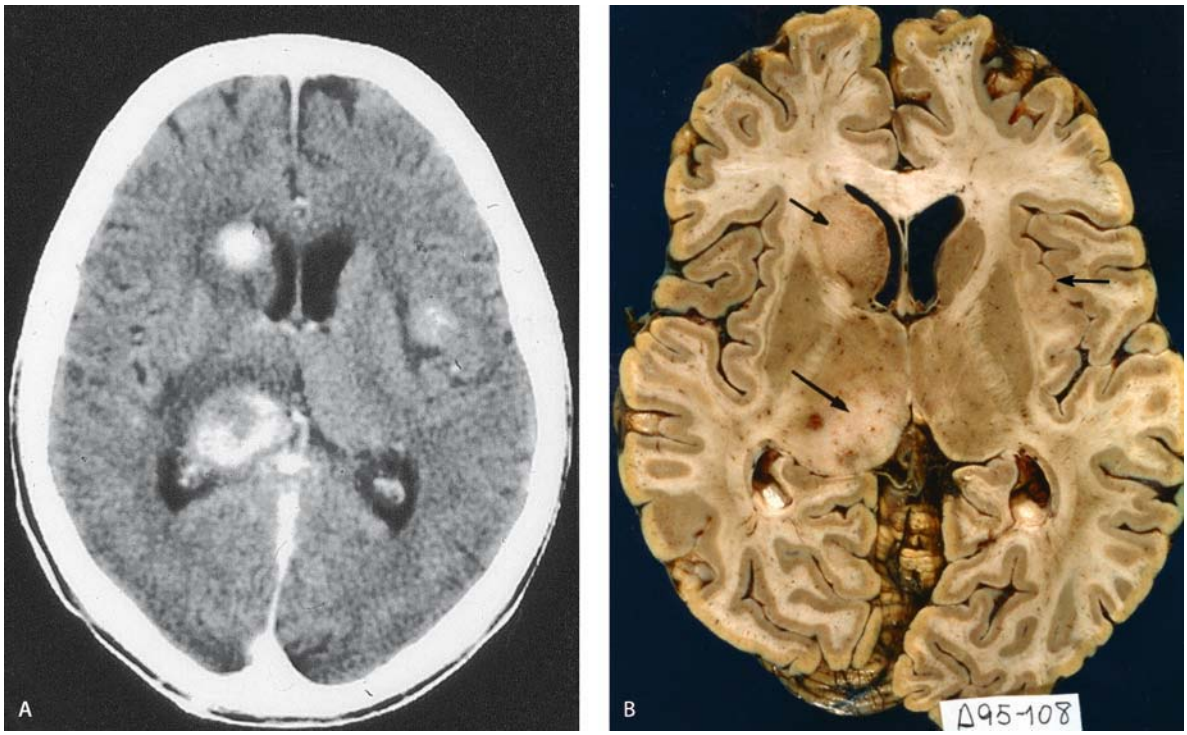

Fig. 27A, B. Primary CNS lymphoma in AIDS patient. **A** Axial contrast-enhanced CECT shows multiples homogeneous enhancing lesions in the right caudate nucleus, left thalamus and left sylvian fissure. **B** Right caudate and thalamus nuclei show a definite pale homogeneous space-occupying mass with ill-defined outlines. Left claustrum is blurred (*arrows*)

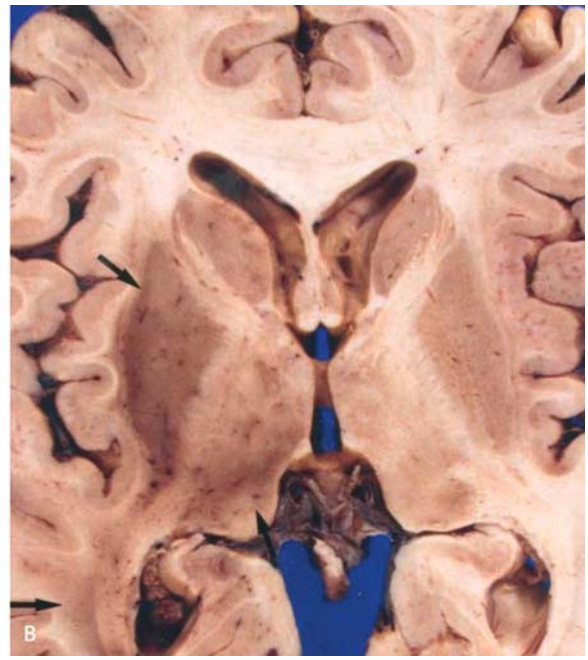

Fig. 28A, B. Nonenhancing primary CNS lymphoma. **A** Axial T2-weighted image shows multiple high-intensity areas in both hemispheres (caudate nucleus, putamen, internal capsula). **B** A rare case of extensive diffuse lymphoma in which the brain appears virtually normal grossly. Left nuclei and deep regions show a darker brownish appearance (*arrow*)

tion (commonly toxoplasma) in AIDS patients. Neoplasms demonstrate increased uptake of thallium, due to their metabolic activity, whereas infection does not. A positive T1 brain SPECT study strongly suggests lymphoma in a patient with AIDS, and biopsy is obtained for confirmation [63].

Radiological studies revealed multiple lesions in 16% of cases, but the true prevalence of multiple lesions proved at pathological examination is 20%–44% [6]).

Metastasis

In the context of this study, metastasis refers to tumors involving the CNS that originate from, but are discontinuous with, primary systemic neoplasms. Solitary or multiple deposits of secondary neoplasms may occur in the CNS parenchyma and cause symptoms of increased intracranial pressure, focal neurological deficit, and epilepsy.

Intracranial spread of tumor is a relatively common occurrence, and metastases are found in approximately 25% of all patients who die from cancer. The initial sources of CNS metastasis are lung, breast, gastrointestinal tract and malignant melanoma. The supratentorial compartment is the most common site, accounting for 80%–85% of metastatic foci. Eighty percent of brain metastases are located in the arterial border zones of the cerebral hemispheres.

Radiopathological Correlation

Metastatic neoplasms form spherical masses in the brain and surrounding edema is evident. The deposit may be firm or have a soft, mucoid or necrotic center. Hemorrhagic deposits are characteristic of melanoma, choriocarcinoma, lung and adenocarcinoma. Malignant melanoma may show obvious pigmentation.

On CT study, the majority of metastases are isodense in comparison to the adjacent brain. Hyperdense metastases are seen with small round cell tumors or hemorrhage (Fig. 29A, B). Cystic metastases are uncommon (Fig. 29E, F). Edema associated with metastasis can be striking and, in some cases, it is the only abnormality seen. After contrast administration, parenchymal metastasis enhances strongly and solid (Fig. 29C, D, G, K) and ring-like patterns are common [71].

On MRI the signal characteristics of metastatic tumors are also variable. Nonhemorrhagic metastases are slightly hypointense in relation to the normal brain tissue on the T1-weighted images. Certain nonhemorrhagic metastatic tumors such as malignant melanoma

Fig. 29A–H. Metastasis. **A**, **B** Acute hemorrhagic metastasis. **C**, **D** Melanoma metastasis. **E**, **F** Intestinal adenocarcinoma metastasis with a cystic mucinous component. **G**, **H** Miliary bronchial carcinoma metastasis

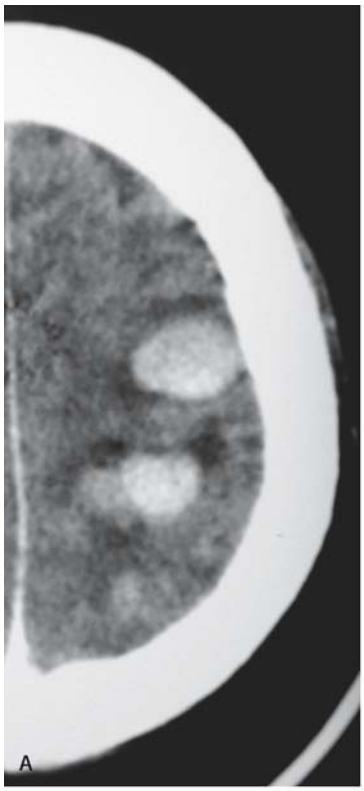
A

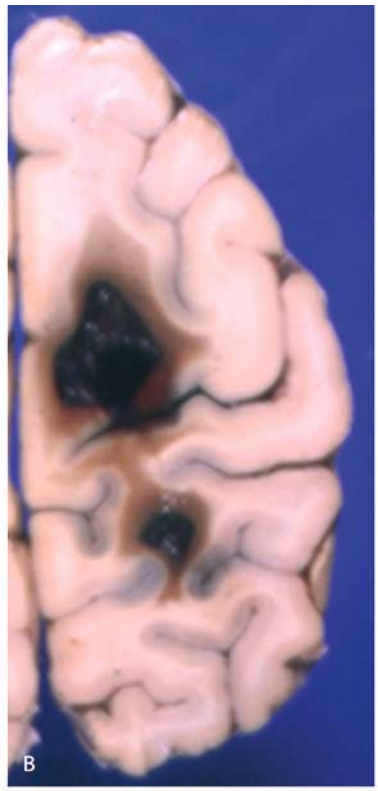
B

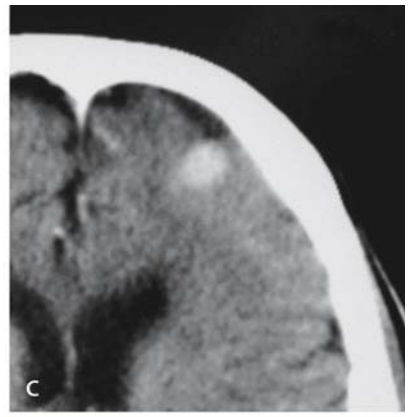
C

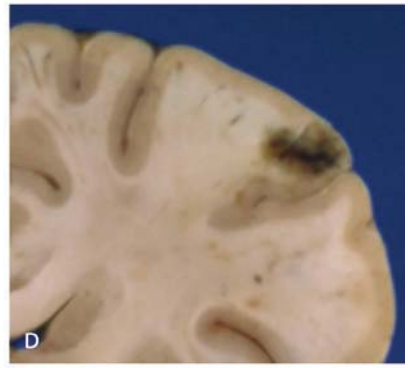
D

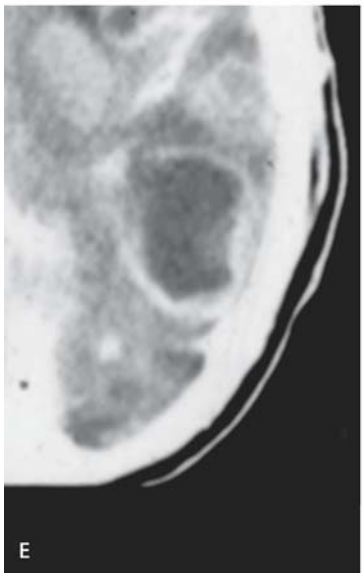
E

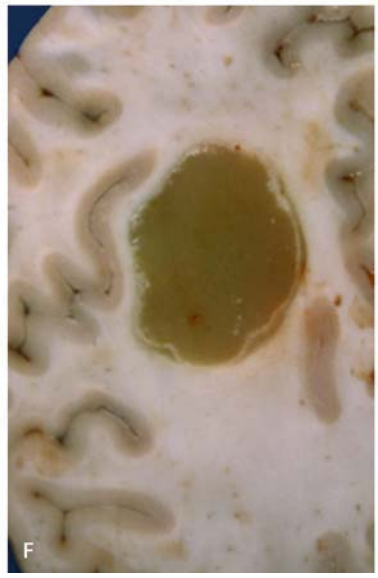
F

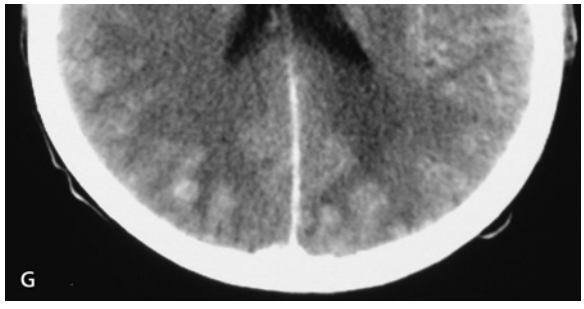
G

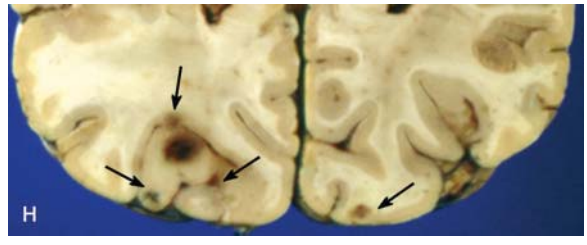
H

are often hyperintense on T1-W. Generally metastases appear as hypointense on T1- and hyperintense on T2-weighted images, with markedly enhanced adjacent parenchymal edema. Solid, rim and mixed patterns occur.

Emerging CNS Neoplasms

Since the appearance in 2000 of the WHO classification for central nervous system neoplasms, numerous descriptions of new entities or variants have appeared in the literature. In the group of neuronal and mixed glioneuronal tumors are lesions with distinctive morphological features that are still not included in a precise classification, including extraventricular neurocytoma, papillary glioneural tumors ad dysembryoplastic-like tumor of the septum pellucidum [72].

Extraventricular Neurocytomas

Extraventricular neurocytomas (EVNS) are mentioned but not formally listed in 2000 WHO classification of tumors of the CNS. Nonetheless, reports of such lesions are increasing and recent studies have better delineated their clinicopathological features [73, 74].

Extraventricular neurocytic neoplasms (Fig. 30) that arise within central nervous system parenchyma share histological features with the most common central neurocytoma, but exhibit a wider morphological spectrum. Neurocytes most often demonstrate finely granular, slight eosinophilic cytoplasm. Less often than their intraventricular counterpart, they exhibit cytoplasmic clearing, which in combination with round nuclei suggest a diagnosis of oligodendroglioma. With regard to biological behavior, like central neurocytoma, most EVNSs are well differentiated and do not recur, especially after complete resection.

Papillary Glioneural Tumors

This uncommon lesion is uniquely characterized by pseudopapillary structures of hyalinized blood vessels surrounded by astrocytic cells.

This tumor occurs in patients of various ages and there is no gender predilection. Occurrence in young children as well as in elderly persons has been observed [13, 14]. The tumors present radiographically as contrast-enhancing cystic masses of variable size, affecting the cerebral hemispheres with no specific location [75].

Follow-up data indicate no evidences of recurrence in tumor totally resected grossly during intervals ranging from 6 months to 7 years [75–77].

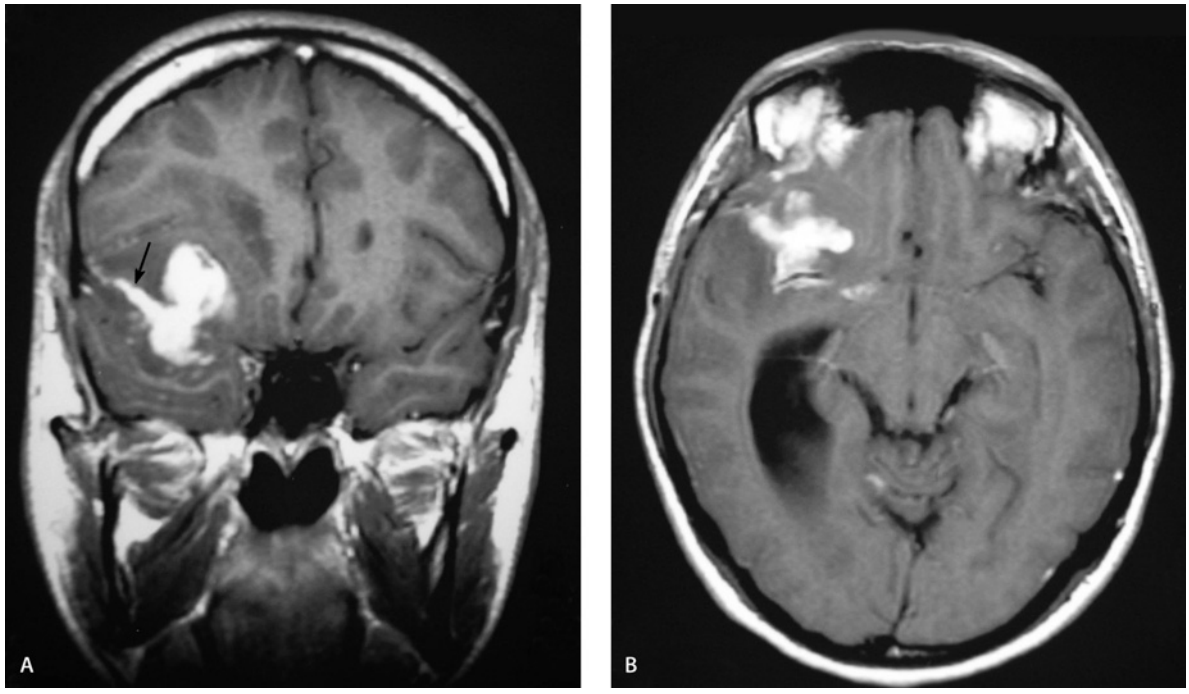

Fig. 30A, B. Extraventricular neurocytoma. Coronal and axial T1-weighted MRI after contrast administration shows enhancing mass arising in the sylvian fissure (*arrow*)

DNT-Like Tumor of the Septum Pellucidum and Caudate Nucleus Area

The DNT tumor is now a well-known, seizure-producing entity that occurs characteristically in the cerebral cortex of children and young adults.

Most recently, DNT-like lesions have been reported to occur in the extracortical locations [78]. The better-characterized location of such DNT-like lesions is the caudate nuclei/septum pellucidum area [79, 80]. As a consequence of this location, the presenting symptoms are those increasing intracranial pressure, in contrast to

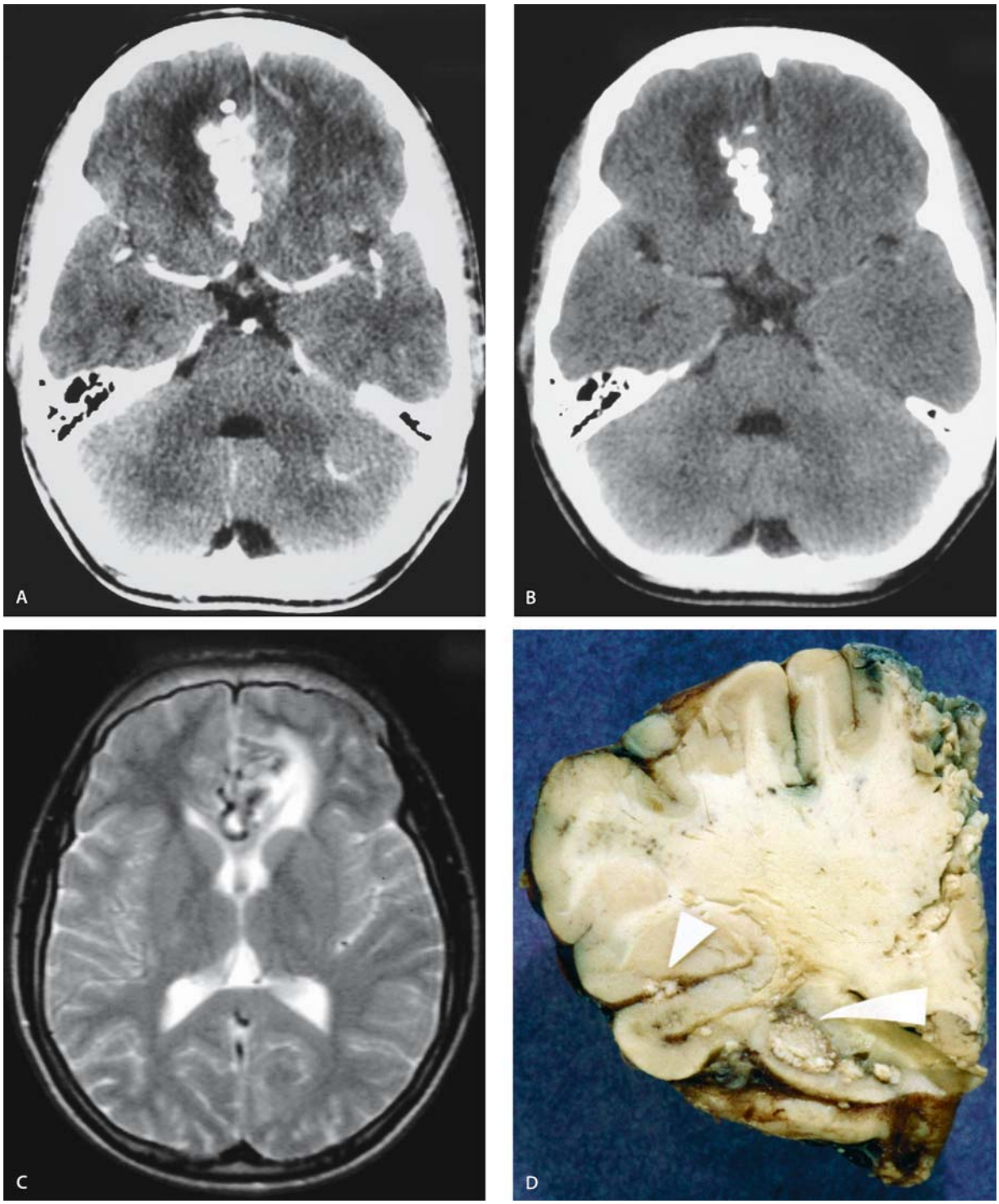

Fig. 31. A–D

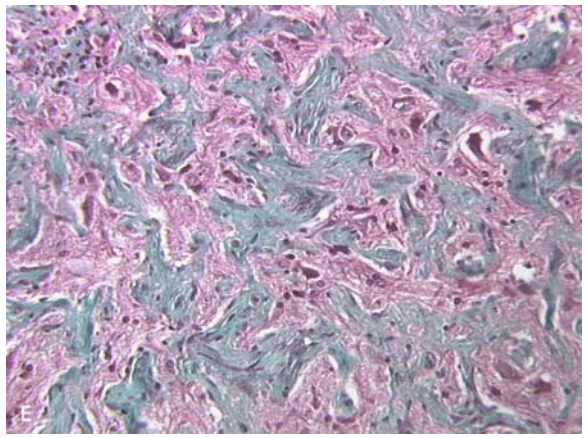

Fig. 31. A–E CT. Gyral calcifications located in frontal cortex of interhemispheric fissure. Hypodense area. **B** Contrast-enhanced CT shows enhancing surrounding area of calcification with invasion of the left frontal lobe. **C** Coronal T1-weighted MRI demonstrates cystic component and areas of flow void. **D** Frontal lobe shows large cortical calcifications (*white arrowheads*). **E** Diffuse cortical meningioangiomatosis. Predominance of meningothelial cells is seen (*green in trichrome staining*)

the seizures observed in the classic intracortical counterpart.

Radiopathological Correlation

Radiographically, the tumors extend in the lateral ventricle from the septal region and obstruct the foramen of Monro, causing varying degrees of hydrocephalus. The lesions are lobular, well-delineated, hypointense on T1-weighted images and hyperintense on T2-weighted images and no enhancing. The histological features include a mucin-rich background, oligodendrocyte-like cells, so-called floating neurons, specific glioneural elements. Distinction from more aggressive neoplasms such as oligodendrogliomas or well-differentiated, diffuse astrocytoma is mandatory because these tumors appear to behave in the benign fashion, similar to that of cortical DNTs [80].

Meningioangiomatosis

Meningioangiomatosis (MA) is a focal lesion of the leptomeninges and underlying cortex, was originally described in association with von Recklinghausen's disease (neurofibromatosis, NF) and has since been known to also occur sporadically [81]. Sporadically MA is fours times more common than MA with NF. MA presents clinically as partial seizures that are difficult to control or as an incidental finding in individuals who are asymptomatic.

Radiopathological Correlation

All patients' MA lesions were confined to the cortex, with variable involvement of the overlying leptomeninges characterized by leptomeningeal and meningovascular proliferation. Cases were classified into those with predominantly cellular and those with predominantly vascular lesions.

Patients with and without NF had similar findings on the various imaging modalities. The commonest finding on CT scan was a calcified enhancing lesion with surrounding low density (Fig. 31) [82]. MRI showed low or mixed central signal on T1 and T2-W in 84% of cases. Gadolinium enhancement is frequently. MA resembled various diseases on MRI, including meningioma, acute hemorrhage, and calcified arteriovenous malformation [81, 83].

Proton MR Spectroscopy (^{1}H MRS) in the Diagnosis of Brain Tumors

Astrocytic Tumors (Low-Grade Astrocytoma, Anaplastic Astrocytoma and Glioblastoma)

In this group, glioblastomas are characterized by the presence of lipids at 0.90 ppm and 1.30 ppm, due to the presence of necrosis [84–87] (Fig. 32). Although a certain amount of lipids can be found in anaplastic astrocytomas, the level of lipids in this group uses to be lower than in glioblastoma. An increase in Cho has been considered to correlate with malignancy in astrocytic tumors. This rule is prevalent for the comparison between anaplastic and low-grade astrocytomas (Figs. 33, 34). Different results are found in the comparison between anaplastic astrocytoma and glioblastoma. Although, in theory, Cho should be higher in glioblastomas, some authors have found lower levels in this group than in anaplastic astrocytomas. A suggested explanation has been a preponderance of necrotic areas over viable proliferative cellular areas in glioblastoma. Lactate has also been considered to correlate with malignancy by some groups; nevertheless values of lactate show a high variability between tumors and cannot be used to differentiate between groups.

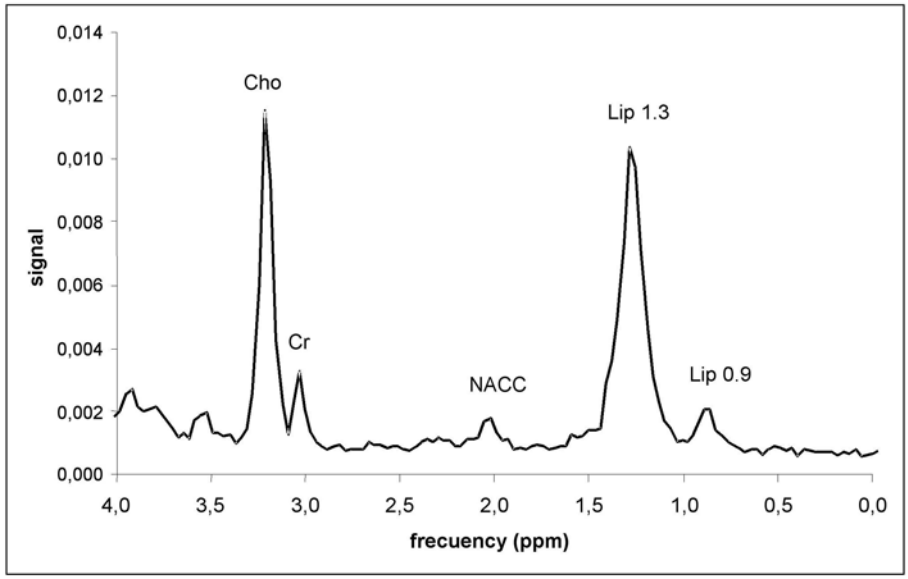

Fig. 32. Mean spectrum of glioblastoma at TE, 136 ms. Lipid resonances correspond to presence of necrosis, characteristic of this tumor

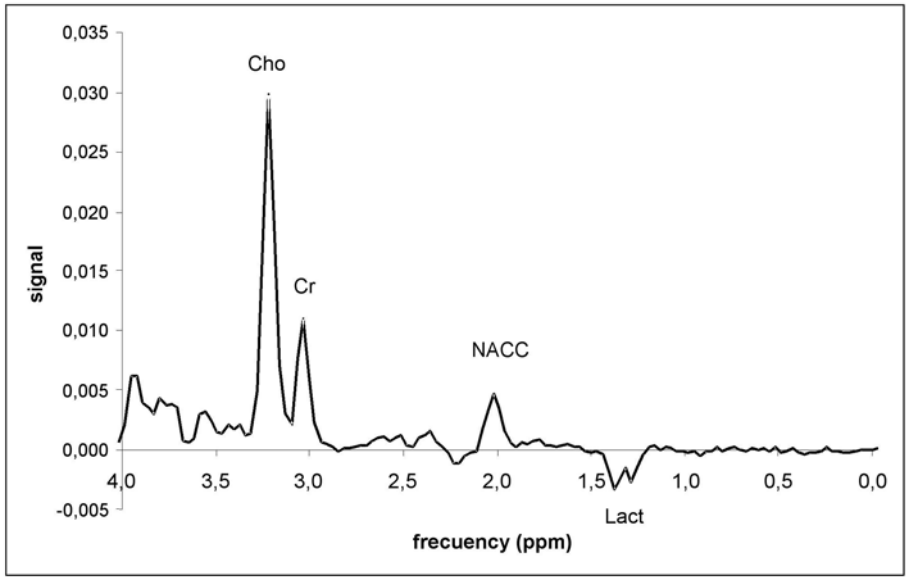

Fig. 33. Mean spectrum of anaplastic astrocytoma at TE, 136 ms. The Cho/Cr ratio is significantly increased. There is also some amount of lactate

Metastasis

Metastases are high-grade brain lesions in which presence of necrosis, represented in the spectrum by broad resonances centered at 0.90 ppm (Lip 0.9) and 1.30 ppm (Lip 1.3) can be found [88]. High values of Cho and low levels of Cr and NACC are also found in this group of tumors (Fig. 35). Differentiation between this group and glioblastoma cannot be confidently made by ^{1}H MRS to date. The origin of metastasis can not be satisfactorily differentiated by ^{1}H MRS either.

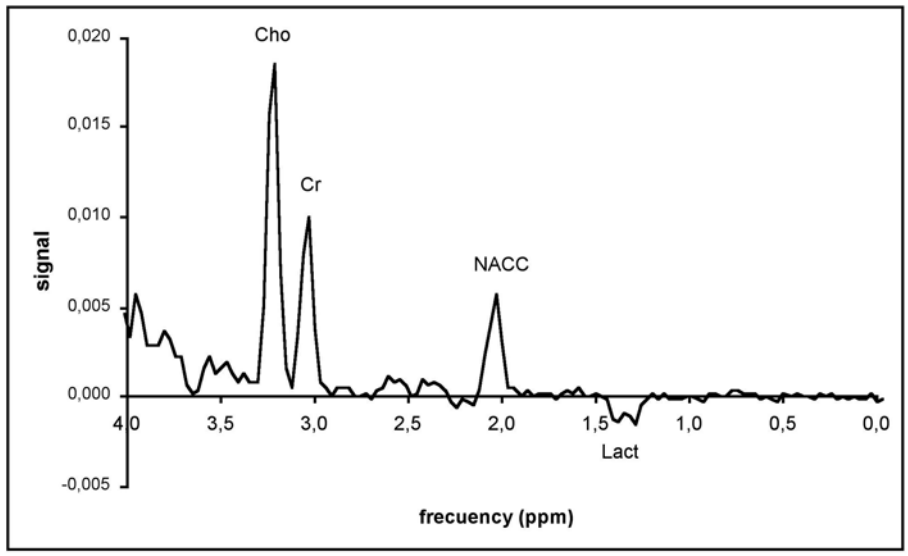

Fig. 34. Mean spectrum of low-grade astrocytoma at TE, 136 ms. There is an increase in the Cho/Cr and Cho/NACC ratios with respect to normal brain, but in lower levels than in anaplastic astrocytoma and meningioma. There is also some amount of lactate

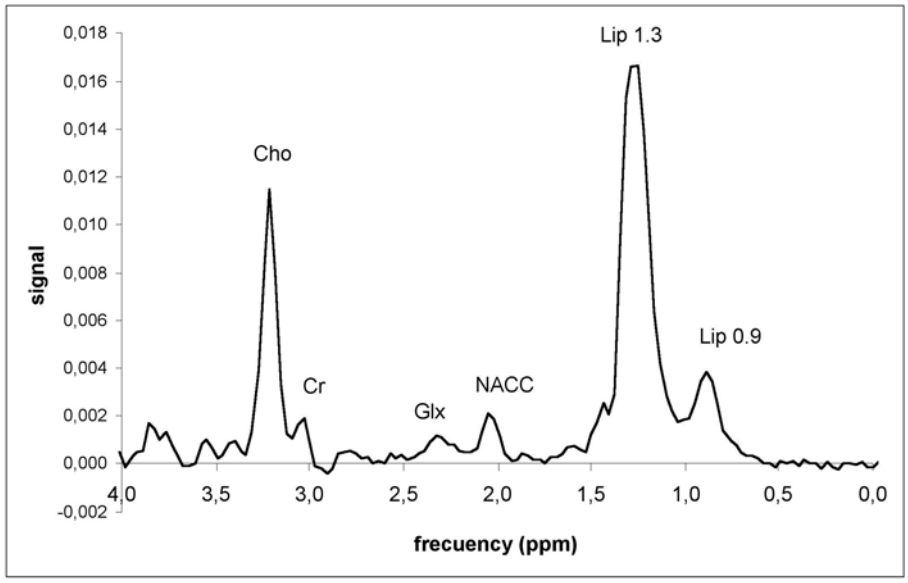

Fig. 35. Mean spectrum of metastasis at TE, 136 ms. The most prevalent findings are high amounts of lipids and Cho, and low levels of NACC and Cr. The spectrum is very similar to glioblastoma

References

1. Kleihues P, Cavance WK (2000) World Health Organization classification of tumours of nervous system. WHO/IARC, Lyon, France
2. Kepes JJ, Rubintein LJ, Enj IE (1979) A distinctive meningocerebral glioma of young subjects with relative favorable prognosis. Cancer 44:1839–1852
3. Housson J, Gambarelli D, Grisoli F, Pellet W, Salomon G, Pellisier J, Toga M (1982) Central neurocytoma. An electron microscopic study of two cases. Acta Neuropathol 56:151–156
4. Daumas-Duport C, Monsaingeon V, Veudoenne C, Munari C, Bancand J, Chodkiewicz JP (1988) Complex neuroepithelial tumors in epilepsy surgery. A series of 20 cases. In: Broggi G, The Rational Basis of Epilepsies, John Libbe, London, pp 149–167
5. Tarauto AL, Monges J, Lylyk P, Leiguatda R (1984) Superficial central astrocytoma attached to dura. Report of six cases in infants. Cancer 54:2505–2512
6. Kleihues P, Cavenee WK (1997) Tumors of the nervous system. IARC Press, Lyon, France, pp 1–225
7. Ellison D, Love S (1998) Astrocytic neoplasms, In Neuropathology, Mosby International, Barcelona, pp 35.1–35.15

8. Dean BL, Drayer , Bird CR et al (1990) Gliomas: Classification with MR imaging. Radiology 174:411–415
9. Castillo M, Seatliff JH, Buldin TW, Sowki K (1992) Radiologic-pathologic correlation: intracranial astrocytomas. AJNR 13: 1609–1661
10. Teronen O, Forbes G, Scheihauter BW, Dietz MJ (1992) Diffuse fibrillary astrocytoma correlation MRI features with histopathologic parameter and tumor grade. Neuroradiology 34: 173–178
11. Barker FG, Chang SM, Huhn SL, Davis RL, Gutin PH, McDermot MW, Wilson CHB (1997) Age and risk of anaplasia in MR nonenhancing supratentorial cerebral tumors. Cancer 80: 936–941
12. Burger PC, Heinz ER, Shih Bata T, Kleihues P (1988) Topographic anatomy and TC correlations in the untreated glioblastoma multiforme. J Neurosurg 68:698–704
13. Rees JH, Smirniotopoulos JG, Jones RV, Wang K (1996) Glioblastoma multiforme: radiopathologic correlations. Radiographic 16:1413–1438
14. Graff PA, Albright AL, Paig D (1992) Dissemination of supratentorial malignant glioma via cerebrospinal fluid in children. Neuroradiology 30:64–71
15. Osborn AG (1994) Brain tumors and tumorlike process. In: Diagnostic neuroradiology. Mosby-Yearbook, St Louis, pp 529–578
16. Hayashi K, Ohara N, Leon HJ, Akagi S, Takahasi , Akagi T, Namiba S (1993) Gliosarcoma with features of chondroblastic osteosarcoma. Cancer 72:850–855
17. Mauri F, Stella L, Benvenuti D, Giamundo A, Pettinati G (1990) Cerebral gliosarcoma: correlation of CT findings, surgical aspect, pathological features, and prognosis. Neurosurgery 26: 261–267
18. Jack CR, Bhausali DT, Chason JL, Boulos RS, Metha BA, Patel SC, Sanders WP (1987) Angiographic features of gliosarcoma. AJNR 8:117–122
19. Clark GB, Hury JM, Mckeever PE (1985) Cerebral pilocytic astrocytoma. Cancer 56:1128–1133
20. Forsth PA, Shaw EG, Schutauer BW, O´Fallon JR, Layton DD Jr, Kazman JA (1993) Supratentorial pilocytic astrocytomas. A clinicopathologic prognosis and flow cytometric study of 51 cases. Cancer 72:1335–1342
21. Katsetos CD, Kristina L (1994) Lobar pilocytic astrocytoma of the cerebral hemispheres: diagnostic and nosology. Clin Neuropathol 13:295–305
22. Palma L, Guidetti B (1985) Cystic pilocytic astrocytomas of the cerebral hemispheres. Surgical experience with 51 cases and long-term results. J Neurosurg 62:811–815
23. Fulhan MJ, Melisi JW, Nishimiya J, Dwyer AJ, Di Chiro G (1993) Neuroimaging of juvenile pilocytic astrocytoma: CT and MRI characteristics. AJNR 152:1263–1270
24. Lee YY, Van Tassel P, Bruner JM, Moser RP, Share JC (1989) Juvenile pilocytic astrocytoma: CT and MRI characteristics. AJR Am J Roentgenol 152:1263–1270
25. Strong JA, Hatlen HP, Brown MT, Debatin JF, Friedman HS, Oakes WJ, Tien R (1993) Pilocytic astrocytoma: correlation between the initial imaging features and clinical aggressiveness. AJR 161:369–372
26. Giannini C, Scheithauer (1997) Classification and grading of low-grade astrocytic tumors in children. Brain Pathol 7: 785–798
27. Russo CP, Frederickson K, Smoker WRK, Ghatok, Naidich TP, Rubin D, Gonzalez-Arias S (1996) Pleomorphic xanthoastrocytoma. J Neuroradiol 2:570–578
28. Turgut M, Akalan N, Ozgen T et al (1996) Subependymal glial cells astrocytoma associated with tuberous sclerosis: diagnosis and surgical characteristics of five cases with unusual features. Clin Neurol Neurosurg 98:217–221
29. Lipper MH, Eberhard DA, Phillips CD (1993) Pleomorphic xanthoastrocytoma, a distinctive astroglial tumor. Neuroradiologic and pathologic features. AJNR 14:1397–1404
30. Romero FJ, Ortega A, Coscojuela P, Rovira A, Ibarra B (1995) Neuroradiological findings in pleomorphic xanthoastrocytoma: report of six cases (abstract). Neuroradiology 37:S88
31. Dolinskas CA, Simeone FA (1982) CT characteristics of intraventricular oligodendrogliomas. AJNR 8:1077–1083
32. Shaw EG, Evans RG, Scheithauer BW, O'Falon JR, Davis DH (1994) Mixed oligoastrocytomas: a survival and prognostic factor analysis. Neurosurgery 24:577–582
33. Armington WG, Osborn AG, Cubberley DA et al (1985) Supratentorial ependymoma: CT appearance. Radiology 175:367–372
34. Swartz JD, Zimmerman RA, Bilaniuk LT (1982) CT of intracranial ependymoma. Radiology 143:97–101
35. Spoto GP, Press GA, Hesselink JR, Salomon (1990) Intracranial ependymoma and subependymoma: MR manifestations AJNR 11:83–91
36. Pleger MJ, Gerson LP (1993) Supratentorial tumors in children. Neuroimaging Clin North Am 3:671–687
37. Maiuri F, Gangemi M, Iaconetta G, (1997) Symptomatic subependymomas the lateral ventricles. Report of eight cases. Clin Neurol Neurosurg 99:17–22
38. Stevens MJ, Kendall BE, Love S (1984) Radiological features of subependymomas with emphasis on computed tomography. Neuroradiology 26:223–228
39. Delfini R, Acqui M, Oppido PA (1991) Tumors of the lateral ventricles. Neurosurg Rev 14:127–133
40. Girardot C, Boukohza M, Lamoureux JP (1990) Choroid plexus papillomas of the posterior fossa in adults: MR imaging and gadolinium enhancement. J Neuroradiol 17:303–318
41. Wagle V, Maclauson D, Eithier R (1987) Choroid plexus papilloma. Magnetic resonance, CT and angiographic observation. Surg Neurol 27:466–468
42. Jeline KJ, Smirniotopoulos JC, Parsi JE, Kanzer M (1990) Lateral intraventricular neoplasms of the brain. AJNR 11:567–574
43. Pizer BL, Moss T, Oakhill A, Webb D, Coakham HB (1995) Congenital astroblastoma: an immunohistochemical study. Case report. J Neurosurg 83:550–555
44. Nevin S (1938) Gliomatosis cerebri. Brain 61:170–191
45. Romero FJ, Ortega A, Titus F, Ibarra B, Navarro C, Rovira M (1988) Gliomatosis cerebri with formation of a glioblastoma multiforme: study and follow-up by MR and CT. J Comput Tomogr 12:253–257
46. Del Carpio OR, Korah I, Salazar A, Melançon D (1996) Gliomatosis cerebri. Radiology 198:830–835
47. Pythien J, Pääkko P (1996) A difficult diagnosis of gliomatosis cerebri: Neuroradiology 38:444–448
48. Ishwar S, Tonoguchi RM, Vogel FS. (1971) Multiple supratentorial hemangioblastomas. Case report and ultrastructural characteristics. J Neurosurg 22:197–203
49. Reyner Y, Baldini M, Hassoun H (1985) Hemangioblastoma of the brain. Computed tomography and angiographic studies in 17 patients. Acta Neurochir 74:12–17
50. Pomper MG, Passer TJ, Burger PC et al (2001) Chordoid glioma: a neoplasm unique to the hypothalamus and anterior third ventricle. AJNR 22:464–469
51. Ricoy JR, Lobato RD, Baez B et al (2000) Suprasellar chordoid glioma. Acta Neuropathol 99:699–703
52. Castillo M, Davis PC, Takei Y, Hoffman JC Jr (1990) Intracranial ganglioglioma: MR, CT and clinical findings in 18 patients. AJNR 11:109–114
53. Tampieri D, Mudgian RM, Melauson D, Either R (1991) Intracranial gangliogliomas in patients with partial complex seizures: CT and MR imaging findings. AJNR 12:749–755
54. Tien RD, Tuosi SL, Pulkinghaums N, Burger PC (1992) Ganglioglioma with leptomeninglial and subarachnoid spread. Result of CT, MR and PET imaging. AJR 159:391–393
55. Vandenberg SR (1993) Desmoplastic infantile ganglioglioma and desmoplastic cerebral astrocytoma of infancy. Brain Pathol 3:275–281
56. Dauma-Duport C (1993) Dysembryoplastic neuroepithelial tumors. Brain Pathol 3:285–295
57. Daumas-Duport C, Scheuthauer BW, Chodkiewicz JP, Laws ER Jr, Vendenne C (1988) Dysembryoplastic neuroepithelial tumor: a surgical curable tumor of young patients with intractable seizures. Report of thirty-nine cases. Neurosurgery 23: 545–556
58. Koeller KK, Dillon WP (1992) Dysembryoplastic neuroepithelial tumors. MR appearance. AJNR 13:1319–1325
59. Kuroiwa T, Bergey GB, Rothman MI, Zoarski LP, Krumholdz A, Barry E (1995) Radiologic appearance of the dysembryoplastic neuroepithelial tumor. Radiology 197:223–238

60. Hassoun J, Söylemezoglu F, Gambarelli D, Figarella-Brauger D, von Amon K, Keihues P (1993) Central neurocytoma: A synopsis of clinical and histological features. Brain Pathol 3:297–306
61. Bolen JW, Lipper MH, Cccano D (1989) Intraventricular neurocytoma. CT and MR findings. A case report. J Comput Assist Tomogr 13:495–497
62. Georgen SK, Gonzañlez MF, McLean CA (1992) Intraventricular neurocytoma. Radiologic features and review of the literature. Radiology 182:787–792
63. Poster-Greenn LM, Silberglest R, Stern H (1991) Intraventricular neuronal neoplasms: CT, MR and angiographic findings. J Comp Assist Tomogr 15.365–368
64. Rorke LB, Trojanowski JO, Lee VMY, Zimmerman RD, Sutlon LN, Biegel JA, Godwein JW, Packer RJ (1997) Primitive neuroectodermal tumors of the central nervous system. Brain Pathol 7:765–784
65. Zimmermam RA (1990) Pediatric supratentorial tumor. Sem Roentgenol 25:225–248
66. Figueroa RE, El Gommal T, Brook BS et al (1989) MR findings on primitive neuroectodermal tumors. J Comput Assist Tomogr 13:773–778
67. Cote TR, Manns A, Hardy CR, Yellin FJ, Harlge P, Yellini FJ (1996) Epidemiology of brain lymphomas among people with or without acquired immunodeficiency syndrome. AIDS/Cancer Study Group. J Natl Cancer Inst 88:675–678
68. Koeller KK, Smirniotopoulous JC, Jones RV (1997) Primary central nervous system lymphoma: radiopathologic correlation. Radiographic 17:1497–1526
69. Whiteman MH, Donovan Post J, Skaler E (1997) Neuroimaging of acquired immunodeficiency syndrome, In: AIDS of the CNS. Lippincott-Raven, Philadelphia
70. Terae S, Ojate A (1996) Nonenhancing primary central nervous system lymphoma. Neuroradiology 38:34–37
71. Osborn AG (1994) Miscellaneous tumors, cysts and metastasis. In: Diagnostic neuroradiology. MosbyYearbook, St Louis, pp 626–670
72. Cenacchi G, Giansgaspero F (2004) Emerging tumor entities and variants of CNS neoplasms. J Neuropathol Exper Neurol 63:185–192
73. Gianspero F, Ceancchi G, Losi L et al (1996) Extraventricular neoplasms with neurocytoma features: a clinicopathological study of 11 cases. Am J Surg Pathol 21:206–212
74. Brat DJ, Scheithauer BW, Eberhart CG, Burger PC (2001) Extraventricular neurocytoma. Pathological features and clinical outcome. Am J Surg Pathol 25:1252–60
75. Komori T, Scheitahauer BW, Anthony DC et al (1998) Papillary glioneural tumor. A new variant of mixed neuronal-glial neoplasm. Am J Surg Pathol 22:1171–1183
76. Payson RA (2000) Papillary glioneural tumours. Arch Pathol Lab Med 20:558–563
77. Broholm H, Madsen FF, Wagner AA, Laursen H (2002) Papillary glioneural tumor. A new tumor entity. Clin Neuropathol 21:1–4
78. Leung SY, Gwi E, Ng HK et al (1994) Dysembryoplastic neuroepithelial tumor. A tumor with small neuronal cells resembling oligodendroglioma. Am J Pathol 18:604–614
79. Cervera-Pierrot P, Varlet P, Chordkiewicz JP, Daumas-Duport C Leung SY, Gwi E, Ng HK et al (1997) Dysembryoplastic neuroepithelial tumor located in the caudate nuclei area: report of four cases. Neurosurgery 40:1065–1070
80. Baiden BL, Brat DJ, Melhem ER, Rosemblum M et al (2001) Dysembryoplastic neuroepithelial tumor-like neoplasm of the septum pellucidum: a lesion often misdiagnosis as glioma. Report of 10 cases. Am Surg Pathol 25:494–
81. Wiebe S, Muñoz DG, Smith S, Lee DH (1999) Meningioangiomatosis. A comprehensive analysis of clinical and laboratory features. Brain 122:709–726
82. Tien RD, Oakes JW, Madden JF, Burger PC (1992) Meningioangiomatosis: CT and MR findings. J Comput Ass Tomograph 16:361–365
83. Aizpuru RN, Quencer RM, Norenberg M, Altman N, Smirniotopoulus J (1991) Radiology (1991) Meningioangiomatosis: clinical, radiologic and histopathologic correlation. 179:819–821
84. Majós C, Alonso J, Aguilera C et al (2003) Proton magnetic resonance spectroscopy (^{1}H MRS) of human brain tumours: assessment of differences between tumour types and its applicability in brain tumour categorization. Eur Radiol 13:582–591
85 Negendank WG, Sauter R, Brown TR et al (1996) Proton magnetic resonance spectroscopy in patients with glial tumors: a multicenter study. J Neurosurg 84:449–458
86. Tien RD, Lai PH, Smith JS et al (1996) Single-voxel proton brain spectroscopy exam (PROBE/SV) in patients with primary brain tumors. AJR Am J Roentgenol 167:201–209
87. Gotsis ED, Fountas K, Kapsalaki E, Toulas P, Peristeris G, Papadakis N (1996) In vivo proton MR spectroscopy: the diagnostic possibilities of lipid resonances in brain tumors. Anticancer Res 16:1565–1568
88. Sijens PE, Knopp MV, Brunetti A et al (1995) 1H MR spectroscopy in patients with metastatic brain tumors: a multicenter study. Magn Reson Med 33: 818–826